

Source Association, DOA, and Fading Coefficients Estimation for Multipath Signals

Wei Xie, *Student Member, IEEE*, Fei Wen, *Member, IEEE*, Jiangbo Liu, *Student Member, IEEE*,
and Qun Wan, *Member, IEEE*

Abstract—This paper addresses the source association (SA), direction of arrival (DOA), and fading coefficients (FCs) estimation problem in multipath environment. First, we establish a rank reduction property for a multipath signal model with the existence of multiple groups of coherent signals. Subsequently, based on this property, effective algorithms for SA, DOA, and FCs estimation have been developed. The proposed DOA and FCs estimation methods exploit the multipath structure information to achieve improved accuracy. The new DOA estimation methods work well even in the case that the DOAs of the multipath signals associated with different sources are (nearly) overlapped. Meanwhile, the new methods are applicable to arbitrary array geometry while without decreasing the effective array aperture. Then, the stochastic Cramér–Rao bound on DOA and FCs estimation of multipath model (MCRB) exploiting the multipath structure information is derived in closed form. Numerical simulations have been provided to demonstrate the effectiveness of the proposed methods.

Index Terms—Cramér–Rao bound, multipath propagation, coherent signals, fading coefficients, direction-of-arrival estimation.

I. INTRODUCTION

DIRECTION-OF-ARRIVAL (DOA) estimation using an array is a fundamental problem in modern signal processing, which has found wide applications in radar, sonar, wireless communications, geophysics, and acoustic tracking [1]–[3]. In the past few decades, this problem has been extensively studied and many methods have been proposed, such as subspace-based approaches [4], [5], sparse-representation based methods [6]–[11], and maximum likelihood (ML) methods (see [1] and references therein).

This work mainly focuses on DOA estimation for coherent signals in multipath environments. In practical multipath

environments, some of the incident signals from distinct directions may be coherent with each other. In this scenario, the popular subspace-based methods can be extended to be applicable by adopting decorrelation preprocessing. For example, forward/backward spatial smoothing (FBSS) [5] and Toeplitz approximation [12] techniques can be used for uniform linear array (ULA), whilst central-symmetric-property based techniques (also known as spatial differencing method [13]) can be used for uniform circular array (UCA) [14] and ULA [15]–[21]. In the spatial differencing based methods [13]–[21], the DOAs of the uncorrelated and coherent signals are estimated separately, and the maximum number of sources processed by these methods can potentially exceed the number of array elements.

These spatial smoothing based methods are simple and efficient, but spatial smoothing would reduce the effective array aperture and lead to performance limitation. To address this problem, the ML methods [22], which have excellent asymptotic and threshold performance, can be applied in the presence of coherent signals. Moreover, the method of direction estimation (MODE) [23], [24], which is derived as large-sample realization of the ML method, and the enhanced principal-singular-vector utilization for modal analysis (EPUMA) [25] are also applicable. In addition, there are a number of sparse-representation based methods proposed recently [6]–[11], which work well in the presence of coherent signals.

Coherency among incident signals is usually considered as a nuisance property for DOA estimation. The main goal of this work is to develop more accurate DOA and fading coefficients (FCs) estimation algorithms via exploiting the coherency structure information in the incident signals. FCs are useful for analyzing the characteristic of multipath channels. In a previous work [26], it has been shown that, based on a coarse DOA estimation and the source association (SA) information obtained via the simple thresholding method [27], DOA and FCs estimation can be improved by exploiting the coherency structure information.

While the work [26] considers ULA and uses a spatial smoothing approach for DOA estimation, the proposed methods in this work apply to arbitrary array geometry without reducing the effective array aperture. Meanwhile, a more generalized scenario, where the signals from distinct sources may arrive at some (nearly) common DOAs, has also been considered in this work. For this generalized scenario, none of the traditional DOA method applies due to resolution limitation. The main contributions are as follows.

Manuscript received April 11, 2016; revised December 29, 2016; accepted January 25, 2017. Date of publication February 15, 2017; date of current version March 24, 2017. The associate editor coordinating the review of this manuscript and approving it for publication was Prof. Marco Lops. This work was supported in part by the National Natural Science Foundation of China under Grant 61401501 and Grant U1533125, in part by the National Science and Technology Major Project under Grant 2016ZX03001022, and in part by the Fundamental Research Funds for the Central Universities under Grant ZYGX2015Z011.

W. Xie, J. Liu, and Q. Wan are with the Department of Electronic Engineering, University of Electronic Science and Technology of China, Chengdu 610054, China (e-mail: raysheik@foxmail.com; jiangbo_liu_uestc@163.com; wanqun@uestc.edu.cn).

F. Wen is with the Department of Electronic Engineering, Shanghai Jiao Tong University, Shanghai 200240, China (e-mail: wenfei@sjtu.edu.cn).

Color versions of one or more of the figures in this paper are available online at <http://ieeexplore.ieee.org>.

Digital Object Identifier 10.1109/TSP.2017.2669894

First, we establish a rank reduction property for multipath signal model (termed as MRARE property). The MRARE property together with the ambiguity properties is the theoretical basis of the new algorithms which can exploit the coherency structure to improve DOA and FCs estimation performance.

Second, based on the MRARE property and a coarse DOA estimation, efficient algorithms for SA, refined DOA and FCs estimation have been developed for two scenarios. 1) In the first one, all the signals are assumed to be well separated, which is a common assumption in traditional methods. In this case, we first propose a combinational optimization based SA estimator, which avoids the parameter selection problem in [27]. Then, the DOAs of each source are refined by multiple one-dimensional (1-D) searching. Finally, the FCs are obtained in closed-form. 2) The second scenario is more generalized in that, the signals of each source are well separated but the signals from distinct sources may arrive at some (nearly) common DOAs. For this generalized case, we propose an algorithm to jointly estimate the SA, refined DOA and FCs by a sequential procedure.

Third, we provide a closed-form expression of the stochastic Cramér-Rao bound (CRB) for DOA and FCs estimation under multipath model, which is termed as MCRB. Furthermore, we provide some analysis on the derived MCRB in comparison with the standard stochastic CRB for DOA estimation [22], termed as GCRB, which does not exploit the multipath structure information. This MCRB has also been analyzed in [26], but it is not concentrated to the only interested DOA and FC block of the parameters.

Finally, various experiments have been conducted to evaluate the new methods in comparison with several state-of-the-art methods. The results demonstrated that the new algorithms can closely approach the MCRB in a wide signal-to-noise ratio (SNR) range and significantly outperform the compared algorithms.

The rest of this paper is organized as follows. Section II introduces the multipath signal model. Section III presents some useful properties of the subspace under multipath signal model. Estimation methods are presented in Section IV. Section V provides a closed-form expression of MCRB and some analysis on the MCRB. Section VI evaluates the proposed methods via simulations. Finally, Section VII concludes the paper.

II. MULTIPATH MODEL

Consider an array with M omni-directional sensors and K far-field narrowband sources located in different azimuth angles $\theta_{11}, \theta_{21}, \dots, \theta_{K1}$. Suppose that the signal emitted by the k -th emitter through P_k paths impinging on the array from distinct directions $\theta_{k1}, \theta_{k2}, \dots, \theta_{kP_k}$, and the corresponding incident signals are $s_{k1}(t), s_{k2}(t), \dots, s_{kP_k}(t)$, respectively. It is assumed that the intersection between the set composed of the DOAs of all the direct signals and the set composed of the DOAs of all the indirect signals is empty. Meanwhile, all the virtual sources are assumed to be far-field and point sources. Without loss of generality, we assume that $P_1 \leq P_2 \leq \dots \leq P_K$ and there are in total D_p sources that through p paths impinging on the array.

Then the total number of incident signals is

$$K_S = \sum_{k=1}^K P_k = \sum_{p=1}^{P_K} p D_p. \quad (1)$$

Based on the above assumptions, the total number of distinct DOAs K_D may be less than K_S .

Suppose that the incident signals corresponding to a same source are coherent with each other [13]. We can write $\mathbf{s}_k(t) = \mathbf{c}_k s_{k1}(t)$, where $\mathbf{s}_k(t) = [s_{k1}(t), s_{k2}(t), \dots, s_{kP_k}(t)]^T$ and $\mathbf{c}_k = [c_{k1}, c_{k2}, \dots, c_{kP_k}]^T$ with c_{kq} and $(\cdot)^T$ denoting the FC of the signal $s_{kq}(t)$ relative to $s_{k1}(t)$ and the transpose operator, respectively. Clearly, we have $c_{k1} = 1$ for any $k \in \{1, 2, \dots, K\}$. The $M \times 1$ array output at time t , denoted by $\mathbf{y}(t)$, can be expressed as

$$\mathbf{y}(t) = \mathbf{B}\mathbf{s}(t) + \mathbf{n}(t), t = 1, 2, \dots, T, \quad (2)$$

where $\mathbf{s}(t) = [s_{11}(t), s_{21}(t), \dots, s_{K1}(t)]^T$, T is the number of snapshots, and $\mathbf{n}(t) \in \mathbb{C}^{M \times 1}$ is additive noise. It is assumed that the noise vector $\mathbf{n}(t)$ is a white Gaussian process with mean zero and covariance $E\{\mathbf{n}(t)\mathbf{n}^H(t)\} = \sigma_n^2 \mathbf{I}_M$, where σ_n^2 , $E\{\cdot\}$, $(\cdot)^H$ and \mathbf{I}_M denote the noise power, expectation operator, conjugate transpose and the $M \times M$ identity matrix, respectively. Moreover, the noise is uncorrelated with $\mathbf{s}(t)$, i.e., $E\{\mathbf{s}(t)\mathbf{n}^H(t)\} = \mathbf{0}$, where $\mathbf{0}$ denotes the matrix of all 0s with a proper size. The matrix $\mathbf{B} = [\mathbf{b}_1, \mathbf{b}_2, \dots, \mathbf{b}_K]$ represents the virtual array manifold, and the virtual steering vector \mathbf{b}_k is a linear combination of the steering vectors corresponding to the k -th source, which can be formulated as

$$\mathbf{b}_k = \mathbf{A}(\boldsymbol{\theta}_k) \mathbf{c}_k \quad (3)$$

with

$$\mathbf{A}(\boldsymbol{\theta}_k) = [\mathbf{a}(\theta_{k1}), \mathbf{a}(\theta_{k2}), \dots, \mathbf{a}(\theta_{kP_k})],$$

where $\boldsymbol{\theta}_k = [\theta_{k1}, \theta_{k2}, \dots, \theta_{kP_k}]^T$ and $\mathbf{a}(\theta)$ is the steering vector of the array towards direction θ .

The array covariance matrix is given by

$$\begin{aligned} \mathbf{R}_Y &= E\{\mathbf{y}(t)\mathbf{y}^H(t)\} = \mathbf{B}\mathbf{R}_S\mathbf{B}^H + \sigma_n^2 \mathbf{I}_M \\ &= \mathbf{A}(\boldsymbol{\eta}_\theta) \mathbf{C}\mathbf{R}_S \mathbf{C}^H \mathbf{A}^H(\boldsymbol{\eta}_\theta) + \sigma_n^2 \mathbf{I}_M, \end{aligned} \quad (4)$$

where $\boldsymbol{\eta}_\theta = [\boldsymbol{\theta}_1^T, \boldsymbol{\theta}_2^T, \dots, \boldsymbol{\theta}_K^T]^T$, $\mathbf{C} = \text{blkdiag}(\mathbf{c}_1, \mathbf{c}_2, \dots, \mathbf{c}_K)$ and $\mathbf{R}_S = E\{\mathbf{s}(t)\mathbf{s}^H(t)\} \in \mathbb{C}^{K \times K}$ is the source covariance matrix. Under the assumption that the source signals are statistically independent and uncorrelated with each other, \mathbf{R}_S is a diagonal matrix consisting of the source signal powers $\sigma_1^2, \sigma_2^2, \dots, \sigma_K^2$.

Based on the received data $\{\mathbf{y}(t)\}_{t=1}^T$ and a coarse DOA estimation, the objective is to determine the SA, a refined DOA estimation and the corresponding FCs. The SA is defined as a set that composed of K elements, where each element in the SA set is a group of DOAs. SA estimation is to classify a coarse DOA estimates into K groups.

From R1 in Section III, the virtual array manifold \mathbf{B} is of full column rank in certain conditions, traditional source number estimation algorithms, such as MDL and AIC [28], can be naturally extended to identify K . Thus, K is assumed to be known

in this paper. In multipath environment, K_D can be estimated by a non-parametric (or semi-parametric) method such as [9] and [29]. However, an implicit assumption used in these methods is that any two distinct DOAs are well separated. In this paper, the basic assumption is that the DOAs corresponding to each source are well separated. Under this relaxed assumption, the DOA separations of some incident signals may be too small to be resolved by the existing methods, and then the estimated value of K_D (denoted by K'_D) may be smaller than the true value of K_D . Nevertheless, the proposed method is capable of handling this circumstance. A more detailed discussion on this point is provided in IV.

III. MRARE PROPERTY

In the presence of multipath propagation, due to the rank deficiency resulting from signal coherency, the signal subspace is no longer spanned by the eigenvectors corresponding to the K_D largest eigenvalues of \mathbf{R}_Y . The methods proposed in [15]–[21] commonly assume that the signal subspace is spanned by the eigenvectors corresponding to the K largest eigenvalues of \mathbf{R}_Y . But this assumption has not been theoretically justified. In the following, we first provide a sufficient condition for this property.

R1: Suppose that the array is unambiguous, and the DOAs of incident signals satisfy the assumption provided in Section II. The virtual array manifold \mathbf{B} is of full column rank when $K_D \leq M$.

Proof: See Appendix A. ■

Denote the eigenvalue decomposition (EVD) of \mathbf{R}_Y by

$$\mathbf{R}_Y = \mathbf{U}_S \mathbf{\Sigma}_S \mathbf{U}_S^H + \mathbf{U}_N \mathbf{\Sigma}_N \mathbf{U}_N^H, \quad (5)$$

where $\mathbf{\Sigma}_S \in \mathbb{R}^{K \times K}$ is a diagonal matrix consisting of the K largest eigenvalues $\{\lambda_k\}_{k=1}^K$, $\mathbf{\Sigma}_N \in \mathbb{R}^{(M-K) \times (M-K)}$ is a diagonal matrix consisting of the $M - K$ smallest eigenvalues $\{\lambda_k\}_{k=K+1}^M$. Provided that the matrix \mathbf{B} is of full column rank, $\mathbf{U}_S \in \mathbb{C}^{M \times K}$ spans the signal subspace whose columns are the eigenvectors corresponding to the K largest eigenvalues and $\mathbf{U}_N \in \mathbb{C}^{M \times (M-K)}$ spans the noise subspace whose columns are the eigenvectors corresponding to the $M - K$ smallest eigenvalues. Then, we have $\text{span}(\mathbf{B}) = \text{span}(\mathbf{U}_S) = \text{null}(\mathbf{U}_N^H)$, and

$$\mathbf{U}_N^H \mathbf{A}(\boldsymbol{\theta}_k) \mathbf{c}_k = \mathbf{0}; k = 1, 2, \dots, K. \quad (6)$$

An important observation follows from (6) is that if

$$M - K \geq \max\{P_1, P_2, \dots, P_K\} = P_K, \quad (7)$$

then $\mathbf{U}_N^H \mathbf{A}(\boldsymbol{\theta})$ is not of full column rank for $\boldsymbol{\theta} \in \{\boldsymbol{\theta}_1, \boldsymbol{\theta}_2, \dots, \boldsymbol{\theta}_K\} \doteq S_t$. Moreover, we have the following result.

R2: Under the assumption of the multipath model in Section II, assume $P_k \leq M - K$ and $K_D \leq M$, then we have

$$\text{rank}(\mathbf{U}_N^H \mathbf{A}(\boldsymbol{\theta}_k)) = P_k - 1. \quad (8)$$

Proof: See Appendix B. ■

From R2, we can construct the following cost function for DOA estimation

$$J_1(\boldsymbol{\theta}, \mathbf{U}_N) = 1/\text{eig}_{\min}(\mathbf{A}(\boldsymbol{\theta})^H \mathbf{U}_N \mathbf{U}_N^H \mathbf{A}(\boldsymbol{\theta})), \quad (9)$$

where $\text{eig}_{\min}(\cdot)$ denotes the minimum eigenvalue. Since different combinations of the elements of a fixed $\boldsymbol{\theta}$ would result in a same value of J_1 , the searching range needs to be restricted, such as by enforcing that the elements of $\boldsymbol{\theta}$ are distinct and in ascending order. This is an implicit condition for all the analysis based on (9) in the following. Interestingly, J_1 does not depend on the unknown FCs, and in the particular case that there exists no multipath, (9) degenerates to the cost function of the classic MUSIC method [4].

Obviously, the cost function (9) may have some false peaks, which would lead to ambiguities in DOA estimation. For example, if we define $\boldsymbol{\theta} = [\boldsymbol{\alpha}^T, \boldsymbol{\beta}^T]^T$, then for any $\boldsymbol{\alpha} \in S_t$ the matrix $\mathbf{U}_N^H \mathbf{A}(\boldsymbol{\theta})$ drops rank. This kind of ambiguity is called type I ambiguity in this paper, which is unfavorable in DOA estimation. However, we find that it still has the following two meaningful properties.

R3: If $P_k + K_D \leq M$, $k \in \{1, 2, \dots, K\}$, then $\boldsymbol{\theta}_k$ must be a local peak of the function J_1 .

Proof: See Appendix C. ■

R4: Assume that $K_D + i \leq M$ ($i = P_1$). The conditions that there exists ambiguity in the i -D space of J_1 are $i > 1$ and at least i' ($i' \geq 2$) sources with i paths. Meanwhile, the DOAs of their indirect signals are the same. When the ambiguous condition is satisfied, the vector $\boldsymbol{\theta}$ that composed by the group of any i distinct DOAs of the i' sources would result in $J_1(\boldsymbol{\theta}, \mathbf{U}_N) = 0$. Meanwhile, the number of ambiguous points brought by these i' sources is $C_{i'+i-1}^i - i'$.

Proof: See Appendix D. ■

The ambiguity discussed in R4 is called type II ambiguity in this paper. Obviously, all the type II ambiguities are composed of true DOAs. For example, supposing $K = 2$, $\boldsymbol{\theta}_1 = [0^\circ, 10^\circ, 20^\circ]^T$ and $\boldsymbol{\theta}_2 = [-10^\circ, 10^\circ, 20^\circ]^T$, only the $C_{2+3-1}^3 - 2 = 2$ type II ambiguities, which are $(-10^\circ, 0^\circ, 20^\circ)$ and $(-10^\circ, 0^\circ, 10^\circ)$, exist in the 3-D space of J_1 .

IV. PROPOSED ALGORITHMS

In this section, we provide practical algorithms for SA, DOA and FCs estimation. Since there may exist DOA ambiguity and the path numbers of sources are unknown, except for some special cases (e.g., $K = 1$ or $K_S = K$), we cannot directly get the DOA estimation from J_1 by a simple searching process. Fortunately, most of the existing methods are capable of providing a coarse DOA estimation even for the generalized case considered in Section IV-B (the DOAs that too close to be separated are treated as one DOA). In the following, the coarse DOA estimation is denoted by $\hat{\boldsymbol{\theta}}^0 \in \mathbb{R}^{K'_D \times 1}$.

Two different scenarios are considered. 1) The well separated case: all the incident signals are well separated. For this case, the SA is firstly estimated by a simple combinational optimization method (see algorithm 1 for detail). Then, based on the SA information, the estimation of DOA and the corresponding FCs are given in Algorithm 2 and (14), respectively. 2) The

generalized case: the incident signals of each source are well separated but the signals from distinct sources may arrive at some (nearly) common DOAs. This case is addressed in Section IV-B. In order to cope with the ambiguity problem in this case, a sequential method (see Algorithm 3) is proposed for joint SA, DOA and FCs estimation.

A. Algorithms for the Well Separated Case

We first consider a simple case that the DOAs of any two incident signals are well separated. In this case, we have $K_S = K_D = K'_D$. When K_D and K are given, the maximum possible path number of one source is $K_D - K + 1$, i.e., $P_k \in \{1, 2, \dots, K_D - K + 1\}$. Although P_1, P_2, \dots, P_K are unknown, the possible combinations of (P_1, P_2, \dots, P_K) can be easily obtained based on the constraint (1). For example, when $K_D = 5$, $K = 2$, there are only two possible combinations, which are (1, 4) and (2, 3). Note that we do not need to consider the order of (P_1, P_2, \dots, P_K) . By R2, we have that, for any true DOA group $\theta \in S_t$, the function $J_2(\theta, \mathbf{U}_N)$ always equals to 0, where $J_2(\theta, \mathbf{U}_N)$ is defined as

$$J_2(\theta, \mathbf{U}_N) = \text{eig}_{\min}(\mathbf{A}(\theta)^H \mathbf{U}_N \mathbf{U}_N^H \mathbf{A}(\theta)). \quad (10)$$

Hence, we have that $J_0(S_t, \mathbf{U}_N) = 0$ also holds, where

$$J_0(S, \mathbf{U}_N) \doteq \sum_{\theta \in S} J_2(\theta, \mathbf{U}_N). \quad (11)$$

Moreover, for a wrong SA, denoted by S_w , we have (see Appendix E)

$$J_0(S_w, \mathbf{U}_N) > 0 \quad (12)$$

when $K_D + P_K \leq M$.

Let N denote the number of possible combinations. Based on the above analysis, we can always find the most probable SA S_n ($n \in \{1, 2, \dots, N\}$) for the n -th possible combination. Among all the N probable SAs, the one minimizes J_0 is selected as the SA estimation. The general lines of the proposed method are described in Algorithm 1.

The most probable SA S_n of the n -th possible combination is identified from step 3 to 9. With the help of the vector $\mathbf{v}^n = [v_1^n, v_2^n, \dots, v_{K_D - K + 1}^n]^T$, the DOA groups are identified one by one (from the source with the minimum path number to the source with the maximum path number), where v_p^n denotes the number of times that p appears in the n -th possible combination. Note that there exists a one to one correspondence between the vectors of $\{\mathbf{v}^n\}_{n=1}^N$ and the possible combinations of (P_1, P_2, \dots, P_K) . In step 7, $\mathbf{a} \setminus \mathbf{b}$ and $\mathbf{a} \subset \mathbf{b}$ denote the vector formed with the elements of the difference set $\{x | x \in S_a \text{ and } x \notin S_b\}$ and the relationship $S_a \subset S_b$, respectively, where the set S_a consists of all the entries of \mathbf{a} and the set S_b consists of all the entries of \mathbf{b} . In step 11, $J_0(S_n, \mathbf{U}_N)$ is calculated as (11). The most probable combination must correspond to the minimum value of J_0 . Consequently, \hat{S} , denoted by $\{\hat{\theta}_k^0\}_{k=1}^K$, is the estimated SA.

When the SA has been estimated, the refined DOA estimation for the k -th ($k \in \{1, 2, \dots, K\}$) source is described in Algorithm 2. The idea is that, starting from the coarse

Algorithm 1: SA Estimation for Well Separated DOAs.

Input: Coarse DOA estimation $\hat{\theta}^0$, $\{\mathbf{v}^n\}_{n=1}^N$ and noise subspace \mathbf{U}_N

- 1: $S_1, S_2, \dots, S_N \leftarrow \emptyset$
- 2: **for** $n \leftarrow 1, 2, \dots, N$ **do**
- 3: $\hat{\theta}^1 \leftarrow \hat{\theta}^0$
- 4: **for** $p \leftarrow 1, 2, \dots, K_D - K + 1$ **do**
- 5: **for** $l \leftarrow 1, 2, \dots, v_p^n$ **do**
- 6: $S_n \leftarrow S_n \cup \arg \min_{\theta \in \mathbb{R}^{p \times 1}, \theta \subset \hat{\theta}^1} J_2(\theta, \mathbf{U}_N)$
- 7: $\hat{\theta}^1 \leftarrow \hat{\theta}^1 \setminus \arg \min_{\theta \in \mathbb{R}^{p \times 1}, \theta \subset \hat{\theta}^1} J_2(\theta, \mathbf{U}_N)$
- 8: **end for**
- 9: **end for**
- 10: **end for**
- 11: Identify the true combination:

$$\hat{n} \leftarrow \arg \min_{n \in \{1, 2, \dots, N\}} J_0(S_n, \mathbf{U}_N)$$

Output: SA estimation: $\hat{S} \leftarrow S_{\hat{n}}$

Algorithm 2: Refined DOA Estimation.

Input: Noise subspace \mathbf{U}_N , coarse DOA estimation of one group $\hat{\theta}_k^0$, searching range δ , maximum number of iteration ι and threshold ε_1

- 1: $l \leftarrow 0$
- 2: **repeat**
- 3: **for** $p \leftarrow 1, 2, \dots, P_k$ **do**
- 4: Update the p -th element of $\hat{\theta}_k^l$:

$$\hat{\theta}_{kp}^{l+1} \leftarrow \arg \max_{\hat{\theta}_{kp}^l \in [\hat{\theta}_{kp}^0 - \delta, \hat{\theta}_{kp}^0 + \delta]} J_1(\hat{\theta}_k^l, \mathbf{U}_N)$$

- 5: **end for**
- 6: $l \leftarrow l + 1$
- 7: **until** $l = \iota$ or

$$\sqrt{\|\hat{\theta}_k^l - \hat{\theta}_k^{l-1}\|_2^2 / P_k} < \varepsilon_1.$$

Output: Refined DOA estimation: $\hat{\theta}_k \leftarrow \hat{\theta}_k^l$

estimation of the k -th source, alternately searching for the local peak in the P_k -D space of J_1 (see step 4 in Algorithm 2). A multiple 1-D searching procedure other than P_k -D searching is used to find the local peak.

Once the DOAs of one group have been refined, the corresponding FCs can be easily calculated based on (6). Specifically, to solve this problem, we use an additional constraint [26]

$$\mathbf{w}_k^T \mathbf{c}_k = 1; k = 1, 2, \dots, K, \quad (13)$$

where $\mathbf{w}_k = [1, \mathbf{0}^T]^T \in \mathbb{R}^{P_k \times 1}$. Let $\bar{\mathbf{c}}_k = [c_{k2}, c_{k3}, \dots, c_{kP_k}]^T$, $k = 1, 2, \dots, K$. The constraint (13) together with (6) results in a closed-form solution as

$$\bar{\mathbf{c}}_k = -(\mathbf{U}_N^H \mathbf{A}'_k)^\dagger \mathbf{U}_N^H \mathbf{a}(\theta_{k1}); k = 1, 2, \dots, K, \quad (14)$$

where $\mathbf{A}'_k = [\mathbf{a}(\theta_{k2}), \mathbf{a}(\theta_{k3}), \dots, \mathbf{a}(\theta_{kP_k})]$ and $(\cdot)^\dagger$ stands for the Moore-Penrose inverse.

B. Algorithms for the Generalized Case

Before deducing the explicit algorithm, we first review the structure of the array covariance matrix. Since the incident signals emitted by different sources are assumed uncorrelated, \mathbf{R}_Y can be rewritten as

$$\mathbf{R}_Y = \mathbf{R}_1 + \mathbf{R}_2 + \dots + \mathbf{R}_{P_K} + \sigma_n^2 \mathbf{I}_M, \quad (15)$$

where \mathbf{R}_p is the part of the array covariance matrix that contributed by the sources with p paths, and the noise power can be estimated as [30]

$$\sigma_n^2 = \frac{1}{M - K} (\lambda_{K+1} + \lambda_{K+2} + \dots + \lambda_M). \quad (16)$$

Let $\mathbf{R}_Y^1 = \mathbf{R}_Y - \sigma_n^2 \mathbf{I}_M$, $D_0 = 0$ and denote the revised array covariance matrices by

$$\mathbf{R}_Y^{p+1} = \mathbf{R}_Y^p - \mathbf{R}_p; p = 1, 2, \dots, P_K - 1. \quad (17)$$

We have

$$\text{rank}(\mathbf{R}_Y^p) = K_p; p = 1, 2, \dots, P_K, \quad (18)$$

where $K_p = K - \sum_{k=0}^{p-1} D_k$ is the number of sources with no less than p paths.

Using the SA information to refine a coarse DOA estimation, we need to identify the DOA groups from $\hat{\boldsymbol{\theta}}^0$ first. Although $J_2(\boldsymbol{\theta}, \mathbf{U}_N) = 0$ still holds when $\boldsymbol{\theta} \in S_t$, there may exist both type I and type II ambiguities, which make the SA estimation problem intractable. Fortunately, by R4, there is no type I ambiguity for $J_2(\boldsymbol{\theta}, \mathbf{U}_N^p)$ when $\boldsymbol{\theta} \in \mathbb{R}^{p \times 1}$, where $\mathbf{U}_N^p \in \mathbb{C}^{M \times (M - K_p)}$ is the noise subspace of \mathbf{R}_Y^p . Thus, the SA estimation problem can be simplified to two subproblems, the estimation of \mathbf{R}_Y^p , $p \in \{1, 2, \dots, P_K\}$ and the identification of the DOA groups with p elements. Clearly, \mathbf{R}_1 only depends on the DOAs, source signal powers and FCs of the sources with one path, where the DOAs can be refined by Algorithm 2 and the FCs can be calculated by (14). Thus, to estimate \mathbf{R}_Y^2 , we only need to identify the DOA groups with one element from $\hat{\boldsymbol{\theta}}^0$ and estimate the corresponding source powers. Then, \mathbf{R}_Y^p ($p > 2$) can be estimated in a similar manner.

Based on the above analysis, we propose a sequential algorithm as described in Algorithm 3. Generally speaking, we first estimate D_p (denoted by \hat{D}_p) and identify all the possible groups with p elements from step 3 to 14, then the corresponding coarse DOAs are refined in step 15, the FCs and source signal powers are estimated in step 16, and the type II ambiguity is eliminated in step 17. Finally, the revised array covariance matrix is updated in step 18. When all the DOA groups have been identified (the stop criterion in step 20 is satisfied), the SA set \hat{S} contains all the estimated DOA groups with a refined estimation.

By R4, only the D_p true DOA groups and the type II ambiguities caused by these true groups satisfy $J_2(\boldsymbol{\theta}, \mathbf{U}_N^p) = 0$ when $\boldsymbol{\theta} \in \mathbb{R}^{p \times 1}$. Hence we can set a threshold ε_2 to the function J_2 to identify all the D_p' DOA groups, where $D_p' (\geq D_p)$ is the summation of D_p and the number of type II ambiguities caused by these D_p true DOA groups. To realize this, we need to list all the possible DOA groups as shown in step 5 (the number of all

Algorithm 3: SA, DOA and FCs Estimation for the Generalized Case.

Input: Coarse DOA estimation $\hat{\boldsymbol{\theta}}^0$, revised covariance matrix \mathbf{R}_Y^1 , threshold $\varepsilon_1, \varepsilon_2$, maximum number of iteration ι and searching range δ

- 1: $\hat{S} \leftarrow \emptyset, p \leftarrow 0$
- 2: **repeat**
- 3: $S' \leftarrow \emptyset, \bar{S}' \leftarrow \emptyset, p \leftarrow p + 1, \hat{D}_p \leftarrow 0$
- 4: $\mathbf{U}_N^p \leftarrow \text{EVD}(\mathbf{R}_Y^p)$
- 5: List all the $I (\doteq C_{K_p}^p)$ possible groups that have p elements from $\hat{\boldsymbol{\theta}}^0: \hat{\boldsymbol{\theta}}'_1, \hat{\boldsymbol{\theta}}'_2, \dots, \hat{\boldsymbol{\theta}}'_I \in \mathbb{R}^{p \times 1}$ (Eq. (19))
- 6: **for** $i \leftarrow 1, 2, \dots, I$ **do**
- 7: **if** $J_2(\hat{\boldsymbol{\theta}}'_i, \mathbf{U}_N^p) \leq \varepsilon_2$ **then** \triangleright detection of DOA groups
- 8: $S' \leftarrow S' \cup \hat{\boldsymbol{\theta}}'_i$ \triangleright candidates of DOA groups
- 9: **if** $\{\hat{\boldsymbol{\theta}}'_{i1}, \hat{\boldsymbol{\theta}}'_{i2}, \dots, \hat{\boldsymbol{\theta}}'_{ip}\} \notin \bar{S}'$ **then**
- 10: $\hat{D}_p \leftarrow \hat{D}_p + 1$ \triangleright estimate D_p
- 11: **end if**
- 12: $\bar{S}' \leftarrow \bar{S}' \cup \{\hat{\boldsymbol{\theta}}'_{i1}, \hat{\boldsymbol{\theta}}'_{i2}, \dots, \hat{\boldsymbol{\theta}}'_{ip}\}$ \triangleright auxiliary set
- 13: **end if**
- 14: **end for**
- 15: Refine DOA estimation of all the groups in S' (Alg. 2)
- 16: Using (14) and (20) to estimate the FCs and source signal powers corresponding to the groups in S' , respectively
- 17: $S'' \leftarrow$ Eliminate type II ambiguities in S' (Eq. (22))
- 18: $\mathbf{R}_Y^{p+1} \leftarrow \mathbf{R}_Y^p - \sum_{l=1}^{D_p} \hat{\sigma}_{pl}^2 \hat{\mathbf{b}}_{pl} \hat{\mathbf{b}}_{pl}^H$
- 19: $\hat{S} \leftarrow \hat{S} \cup S''$
- 20: **until** $\hat{D}_1 + \hat{D}_2 + \dots + \hat{D}_p \geq K$ or $p \geq K_D$

Output: Estimated FCs and SA \hat{S} with refined DOAs

the possible groups is denoted by I), and then the corresponding values of $J_2(\boldsymbol{\theta}, \mathbf{U}_N^p)$ can be directly calculated by (10). If the value of J_2 is smaller than ε_2 , the corresponding group is identified as a candidate. Let the set S' contain all the candidates (it is updated in step 8). The value of D_p' can be easily obtained by counting the elements of S' . However, we need to know the value of D_p . Observe that, based on the assumption of the signal model, all the distinct DOAs in these D_p' groups are contained in any D_p groups of it. Thus, D_p can be obtained with the help of a temporary set \bar{S}' as shown in step 7 to 13 (specifically, it is iteratively estimated in step 10).

There is a problem in estimating D_p . If D_p is greater than 2, all the distinct DOAs of these D_p sources may be contained in less than D_p groups, then the estimated D_p , i.e., \hat{D}_p , may be less than the true value of D_p . For example, if $p = 2$ and there are 3 sources with their true DOA groups are $\{\theta_0, \theta_1\}$, $\{\theta_0, \theta_2\}$ and $\{\theta_0, \theta_3\}$, then the type II ambiguities are $\{\theta_1, \theta_2\}$, $\{\theta_1, \theta_3\}$ and $\{\theta_2, \theta_3\}$. We can see that the two (less than $D_p = 3$) DOA groups $\{\theta_0, \theta_1\}$ and $\{\theta_0, \theta_2\}$ contain all the 4 distinct DOAs. However, we can always find the maximum number of DOA

groups by arranging the sequence of $\{\hat{\boldsymbol{\theta}}'_i\}_{i=1}^I$ in step 5 as

$$\begin{aligned} & \{[\hat{\theta}_1^0, \hat{\theta}_2^0, \dots, \hat{\theta}_p^0, \hat{\theta}_{p+1}^0]^T, [\hat{\theta}_1^0, \hat{\theta}_2^0, \dots, \hat{\theta}_p^0, \hat{\theta}_{p+2}^0]^T, \dots, \\ & [\hat{\theta}_1^0, \hat{\theta}_2^0, \dots, \hat{\theta}_p^0, \hat{\theta}_{K'_D}^0]^T, [\hat{\theta}_1^0, \hat{\theta}_2^0, \dots, \hat{\theta}_{p-1}^0, \hat{\theta}_{p+1}^0, \hat{\theta}_{p+2}^0]^T \\ & , \dots, [\hat{\theta}_{K'_D-p}^0, \hat{\theta}_{K'_D-(p-1)}^0, \dots, \hat{\theta}_{K'_D-1}^0, \hat{\theta}_{K'_D}^0]^T\} \end{aligned} \quad (19)$$

where $\hat{\theta}_k^0$ is the k -th element of $\hat{\boldsymbol{\theta}}^0$.

Next, we show the realization of step 17, i.e., eliminating the type II ambiguities in S' . Before that, we use Algorithm 2 to refine all the DOAs for each of the DOA groups in S' in step 15, and the FCs are estimated by (14) in step 16. Meanwhile, each of the elements in S' corresponds to a virtual steering vector, denoted by $\bar{\mathbf{b}}_i, i = 1, 2, \dots, D'_p$, which can be calculated by (3). It can be easily verified that

$$\text{rank}(\mathbf{R}_Y^p) = \text{rank}(\mathbf{R}_Y^p - \sigma_q^2 \mathbf{b}_q \mathbf{b}_q^H) + 1$$

holds for $q \in \{K - K_p + 1, K - K_p + 2, \dots, K\}$. Hence the signal powers can be estimated as

$$\bar{\sigma}_i^2 = \arg \min_{\sigma^2} \text{eig}_{K_p}(\mathbf{R}_Y^p - \sigma^2 \bar{\mathbf{b}}_i \bar{\mathbf{b}}_i^H), i = 1, 2, \dots, D'_p \quad (20)$$

where $\text{eig}_k(\cdot)$ denotes the k -th eigenvalue. To eliminate the type II ambiguities, we need the following result.

R5: Let $\mathbf{R}'_p = \sum_{i=1}^{D'_p} \bar{\sigma}_i^2 \bar{\mathbf{b}}_i \bar{\mathbf{b}}_i^H$, where $\{l_1, l_2, \dots, l_{D'_p}\} \subset \{1, 2, \dots, D'_p\}$. If \mathbf{B} is of full column rank, we have

$$\text{rank}(\mathbf{R}_Y^p - \mathbf{R}'_p) \geq K_{p+1}, \quad (21)$$

where the equality holds only when the indexes in $\{l_1, l_2, \dots, l_{D'_p}\}$ correspond to the true DOA groups in S' .

Proof: See Appendix F. \blacksquare

Based on R5, the following cost function can be used for identifying the true DOA groups:

$$\Omega' = \arg \min_{\substack{\Omega = \{l_i\}_{i=1}^{D'_p} \\ \Omega \subset \{1, 2, \dots, D'_p\}}} \text{eig}_{K_{p+1}} \left(\mathbf{R}_Y^p - \sum_{i=1}^{D'_p} \bar{\sigma}_i^2 \bar{\mathbf{b}}_i \bar{\mathbf{b}}_i^H \right) \quad (22)$$

where the index set Ω contains the D'_p distinct elements in S' . Let $S'' = S'_\Omega$, which completes the realization of step 17.

Let $\{\hat{\sigma}_{pl}^2\}_{l=1}^{D'_p}$ and $\{\hat{\mathbf{b}}_{pl}\}_{l=1}^{D'_p}$ denote the selected powers and virtual steering vectors from (22), respectively. Clearly, \mathbf{R}_Y^{p+1} can be easily calculated as step 18. In the next iteration, the group identification is not affected by the identified sources. We note that the accuracy of the revised array covariance is affected by the errors in the estimated DOAs, FCs and the signal powers. By R3, a refined DOA estimation can also be obtained by searching the local peak of $J_1(\boldsymbol{\theta}, \mathbf{U}_N)$. Thus, other than $\mathbf{U}_N^p, \mathbf{U}_N (= \mathbf{U}_N^1)$ is preferred as the input of Algorithm 2 in step 15.

From (18), we have $\text{rank}(\mathbf{R}^{P_{K+1}}) = 0$. Thus, for a correct SA estimation, the entries of the output revised array covariance in algorithm 3 should be very small. This observation directly gives rise to a reliability test on algorithm 3. Moreover, the following cost function can be used to obtain a reliable threshold ε_2 :

$$\varepsilon_2 = \min_{\varepsilon} \|\mathbf{R}'(\varepsilon)\|_F, \quad (23)$$

where $\mathbf{R}'(\varepsilon)$ denotes the output revised array covariance with using the threshold ε , and $\|\cdot\|_F$ is the Frobenius norm.

V. CRAMÉR-RAO BOUND (CRB)

In this section, the stochastic CRB for the multipath model (2) with prior information of SA is provided. In this model, the unknown parameters include K_S DOAs $\{\boldsymbol{\theta}_k\}_{k=1}^K$, the real and imaginary parts of $K_S - K$ FCs $\{\Re(\bar{\mathbf{c}}_k), \Im(\bar{\mathbf{c}}_k)\}_{k=1}^K$, the noise variance σ_n^2 and the parameters of the source covariance matrix $\{R_{Skl}\}_{k=1}^K, \{\Re(R_{Skl}), \Im(R_{Skl}); k > l\}_{k,l=1}^K$, where R_{Skl} denotes the (k, l) -th element of \mathbf{R}_S , $\bar{\mathbf{c}}_k$ is defined in (14), $\Re(\cdot)$ and $\Im(\cdot)$ denote the real part and imaginary part operators, respectively. Let us define $\boldsymbol{\eta} \in \mathbb{R}^{(3K_S - 2K) \times 1}$ containing all the interested parameters as

$$\boldsymbol{\eta} = [\boldsymbol{\eta}_\theta^T, \boldsymbol{\eta}_{Rc}^T, \boldsymbol{\eta}_{Ic}^T]^T, \quad (24)$$

where $\boldsymbol{\eta}_\theta$ is defined in (4) and

$$\begin{aligned} \boldsymbol{\eta}_{Rc} &= [\Re(\bar{\mathbf{c}}_1^T), \Re(\bar{\mathbf{c}}_2^T), \dots, \Re(\bar{\mathbf{c}}_K^T)]^T, \\ \boldsymbol{\eta}_{Ic} &= [\Im(\bar{\mathbf{c}}_1^T), \Im(\bar{\mathbf{c}}_2^T), \dots, \Im(\bar{\mathbf{c}}_K^T)]^T. \end{aligned}$$

In order to derive a concise expression, firstly, we augment the DOA vectors $\{\boldsymbol{\theta}_k\}_{k=1}^K$ to $\{\boldsymbol{\theta}'_k = [\boldsymbol{\theta}_k^T, \mathbf{0}^T]^T\}_{k=1}^K$ such that these vectors all have the same size of $P_K \times 1$. Secondly, we augment the FC vectors $\{\Re(\bar{\mathbf{c}}_k), \Im(\bar{\mathbf{c}}_k)\}_{k=1}^K$ to $\{\Re(\hat{\mathbf{c}}'_k), \Im(\hat{\mathbf{c}}'_k); \hat{\mathbf{c}}'_k = [\bar{\mathbf{c}}_k^T, \mathbf{0}^T]^T\}_{k=1}^K$ such that these vectors all have the same size of $(P_K - 1) \times 1$. Then, define an augmented and rearranged vector $\boldsymbol{\eta}' \in \mathbb{R}^{(3P_K K - 2K) \times 1}$ as

$$\boldsymbol{\eta}' = [\boldsymbol{\eta}'_\theta, \boldsymbol{\eta}'_{Rc}, \boldsymbol{\eta}'_{Ic}]^T, \quad (25)$$

where

$$\begin{aligned} \boldsymbol{\eta}'_\theta &= [\theta'_{11}, \theta'_{21}, \dots, \theta'_{K1}, \theta'_{12}, \theta'_{22}, \dots, \theta'_{K P_K}]^T, \\ \boldsymbol{\eta}'_{Rc} &= [\Re(\hat{\mathbf{c}}'_{11}), \Re(\hat{\mathbf{c}}'_{21}), \dots, \Re(\hat{\mathbf{c}}'_{K1}), \\ & \quad \Re(\hat{\mathbf{c}}'_{12}), \Re(\hat{\mathbf{c}}'_{22}), \dots, \Re(\hat{\mathbf{c}}'_{K(P_K-1)})]^T, \\ \boldsymbol{\eta}'_{Ic} &= [\Im(\hat{\mathbf{c}}'_{11}), \Im(\hat{\mathbf{c}}'_{21}), \dots, \Im(\hat{\mathbf{c}}'_{K1}), \\ & \quad \Im(\hat{\mathbf{c}}'_{12}), \Im(\hat{\mathbf{c}}'_{22}), \dots, \Im(\hat{\mathbf{c}}'_{K(P_K-1)})]^T. \end{aligned}$$

Obviously, there exists a selection matrix \mathbf{J} with the size of $(3K_S - 2K) \times (3P_K K - 2K)$ such that

$$\boldsymbol{\eta} = \mathbf{J} \boldsymbol{\eta}'. \quad (26)$$

Based on the stochastic assumption, we have $\mathbf{y}(t) \sim \mathbb{N}(\mathbf{0}, \mathbf{R}_Y)$, where $\mathbb{N}(\cdot, \cdot)$ denotes the complex Gaussian distribution. The log-likelihood function concentrated with respect to the noise variance σ_n^2 and the parameters of the source covariance matrix can be expressed as [22]

$$L(\boldsymbol{\eta}) = \ln \left(\det \left(\mathbf{B} \hat{\mathbf{R}}_S \mathbf{B}^H + \hat{\sigma}_n^2 \mathbf{I}_M \right) \right) \quad (27)$$

with

$$\begin{aligned} \hat{\mathbf{R}}_S &= \mathbf{B}^\dagger \hat{\mathbf{R}}_Y \mathbf{B}^{\dagger H} - \hat{\sigma}_n^2 (\mathbf{B}^H \mathbf{B})^{-1}, \\ \hat{\sigma}_n^2 &= \text{Tr}(P_{\mathbf{B}}^\perp \hat{\mathbf{R}}_Y) / (M - K), \end{aligned}$$

where $\hat{\mathbf{R}}_Y = \sum_{t=1}^T \mathbf{y}(t) \mathbf{y}^H(t) / T$, $P_{\mathbf{B}}^\perp = \mathbf{I}_M - \mathbf{B} \mathbf{B}^\dagger$ and $\text{Tr}(\cdot)$ denotes the trace operator. Meanwhile, we have the following

result [22], [31]:

$$\begin{aligned} [CRB^M(\boldsymbol{\eta})]_{ij}^{-1} &= T \lim_{T \rightarrow \infty} \frac{\partial^2 L(\boldsymbol{\eta})}{\partial \eta_i \partial \eta_j} \\ &= \frac{2T}{\sigma_n^2} \Re \left\{ \text{Tr} \left[\mathbf{U} \frac{\partial \mathbf{B}^H}{\partial \eta_j} P_{\mathbf{B}}^\perp \frac{\partial \mathbf{B}}{\partial \eta_i} \right] \right\} \end{aligned} \quad (28)$$

with

$$\mathbf{U} = \mathbf{R}_S \mathbf{B}^H \mathbf{R}_Y^{-1} \mathbf{B} \mathbf{R}_S.$$

Let us define a matrix $\boldsymbol{\Psi} \in \mathbb{C}^{(3P_K K - 2K) \times (3P_K K - 2K)}$ with its (i, j) -th element

$$[\boldsymbol{\Psi}]_{ij} = \frac{2T}{\sigma_n^2} \Re \left\{ \text{Tr} \left[\mathbf{U} \frac{\partial \mathbf{B}^H}{\partial \eta_j} P_{\mathbf{B}}^\perp \frac{\partial \mathbf{B}}{\partial \eta_i} \right] \right\}, \quad (29)$$

where η'_i is the i -th element of $\boldsymbol{\eta}'$. Then (28) can be rewritten as

$$[CRB^M(\boldsymbol{\eta})]^{-1} = \mathbf{J} \boldsymbol{\Psi} \mathbf{J}^T. \quad (30)$$

After straightforward manipulations using (29) and (30), the CRB matrix can be expressed in a closed-form as

$$\begin{aligned} CRB^M(\boldsymbol{\eta}) &= \frac{\sigma_n^2}{2T} \left\{ \mathbf{J} \Re \left\{ (\mathbf{1}^T \otimes \mathbf{U}) \odot (\mathbf{H}^H P_{\mathbf{B}}^\perp \mathbf{H})^T \right\} \mathbf{J}^T \right\}^{-1} \end{aligned} \quad (31)$$

where $\mathbf{1}$ is a $(3P_K - 2) \times 1$ vector of 1s, \otimes and \odot stand for the Kronecker product and Hadmard product, respectively, and

$$\mathbf{H} = [\mathbf{H}_\theta, \mathbf{H}_{CR}, \mathbf{H}_{CI}] \quad (32)$$

with

$$\begin{aligned} \mathbf{H}_\theta &= [\mathbf{d}(\theta'_{11}), \mathbf{d}(\theta'_{21}), \dots, \mathbf{d}(\theta'_{K1}), \check{c}'_{11} \mathbf{d}(\theta'_{12}), \dots, \\ &\quad \check{c}'_{K1} \mathbf{d}(\theta'_{K2}), \check{c}'_{12} \mathbf{d}(\theta'_{13}), \dots, \check{c}'_{K(P_K-1)} \mathbf{d}(\theta'_{KP_K})], \end{aligned}$$

$$\mathbf{H}_{CR} = [\mathbf{a}(\theta'_{12}), \mathbf{a}(\theta'_{22}), \dots, \mathbf{a}(\theta'_{K2}), \mathbf{a}(\theta'_{13}), \dots, \mathbf{a}(\theta'_{KP_K})],$$

$$\mathbf{H}_{CI} = j \mathbf{H}_{CR},$$

where $\mathbf{d}(\theta) = \partial \mathbf{a}(\theta) / \partial \theta$.

Since we use an additional prior of the structure of multipath channels, intuitively, MCRB should be lower than or at least equal to the GCRB [22]. This is verified by simulations in Section VI-B. However, we failed to prove such a conjecture mathematically for a generalized situation. In the following, two special conditions for the equivalence between the MCRB and GCRB are provided.

The GCRB, denoted by $CRB^G(\boldsymbol{\eta}_\theta)$, can be expressed as [22]

$$\begin{aligned} CRB^G(\boldsymbol{\eta}_\theta) &= \frac{\sigma_n^2}{2T} \left\{ \Re \left\{ \mathbf{U}' \odot \left(\mathbf{D}^H(\boldsymbol{\eta}_\theta) P_{\mathbf{A}(\boldsymbol{\eta}_\theta)}^\perp \mathbf{D}(\boldsymbol{\eta}_\theta) \right)^T \right\} \right\}^{-1}, \end{aligned} \quad (33)$$

where

$$\mathbf{U}' = \mathbf{C} \mathbf{R}_S \mathbf{C}^H \mathbf{A}^H(\boldsymbol{\eta}_\theta) \mathbf{R}_Y^{-1} \mathbf{A}(\boldsymbol{\eta}_\theta) \mathbf{C} \mathbf{R}_S \mathbf{C}^H$$

and $\mathbf{D}(\boldsymbol{\eta}_\theta) = [\mathbf{d}(\theta_{11}), \dots, \mathbf{d}(\theta_{1P_1}), \mathbf{d}(\theta_{21}), \dots, \mathbf{d}(\theta_{KP_K})]$. Note that the GCRB expression (33) needs an appropriate modification when $K_D < K_S$.

Condition 1: The incident signals are not coherent with each other (i.e., $K_S = K$).

In this case, we have $\mathbf{C} = \mathbf{I}_K$, $\mathbf{J} = \mathbf{I}_K$, $\mathbf{H} = \mathbf{H}_\theta = \mathbf{D}(\boldsymbol{\eta}_\theta)$, $\mathbf{B} = \mathbf{A}(\boldsymbol{\eta}_\theta)$ and $\boldsymbol{\eta}_\theta = [\theta_{11}, \theta_{21}, \dots, \theta_{K1}]^T$. Consequently, (31) reduces to (33).

Condition 2: There is only one source, i.e., $K = 1$.

The proof of this condition is not as obvious as condition 1. To prove this condition, we need the following result.

R6: If $K = 1$, the DOA block $CRB^M(\boldsymbol{\eta}_\theta)$ in $CRB^M(\boldsymbol{\eta})$ is given by

$$CRB^M(\boldsymbol{\eta}_\theta) = \frac{\sigma_n^2}{2Tu} \left\{ \Re \left\{ \left(\mathbf{H}_\theta^H P_{\mathbf{A}(\boldsymbol{\eta}_\theta)}^\perp \mathbf{H}_\theta \right)^T \right\} \right\}^{-1} \quad (34)$$

where $u = \sigma_1^4 \mathbf{b}_1^H \mathbf{R}_Y^{-1} \mathbf{b}_1 \in \mathbb{R}^{1 \times 1}$ and the DOA vector $\boldsymbol{\eta}_\theta = [\theta_{11}, \theta_{12}, \dots, \theta_{1P_1}]^T$.

Proof: See Appendix G. ■

Proof of condition 2: It follows from (34) and (33) that, the (i, j) -th elements of $[CRB^M(\boldsymbol{\eta}_\theta)]^{-1}$ and $[CRB^G(\boldsymbol{\eta}_\theta)]^{-1}$ can be expressed as

$$\frac{2T}{\sigma_n^2} \Re \left\{ \left(\sigma_1^4 \mathbf{b}_1^H \mathbf{R}_Y^{-1} \mathbf{b}_1 \right) \left(c_{1i} \mathbf{d}^T(\theta_{1i}) P_{\mathbf{A}(\boldsymbol{\eta}_\theta)}^{\perp T} \mathbf{d}^*(\theta_{1j}) c_{1j}^* \right) \right\} \quad (35)$$

and

$$\frac{2T}{\sigma_n^2} \Re \left\{ U'_{ij} \left(\mathbf{d}^T(\theta_{1i}) P_{\mathbf{A}(\boldsymbol{\eta}_\theta)}^{\perp T} \mathbf{d}^*(\theta_{1j}) \right) \right\}, \quad (36)$$

respectively, where the (i, j) -th element of \mathbf{U}' is given by

$$U'_{ij} = \sigma_1^4 c_{1i} c_{1j}^* \mathbf{b}_1^H \mathbf{R}_Y^{-1} \mathbf{b}_1. \quad (37)$$

Clearly, substituting (37) back into (36), (35) and (36) have an identical expression, which completes the proof. ■

VI. SIMULATIONS

In this section, the performance of the proposed algorithms are evaluated in comparison with several representative algorithms and the MCRB. The comparison between MCRB and GCRB under different conditions is also provided. The coarse DOA estimation in section VI-C and VI-D is obtained by the iterative reweighted least square (IRLS) version of MSBL (denoted by MSBL-IRLS) [32], [33]. It turns out that MSBL-IRLS has a faster convergence rate than the original MSBL algorithm [11], meanwhile, maintains a good performance. We evaluate the DOA and FCs estimation performance in terms of root-mean-squared-error (RMSE), which is defined as

$$\text{RMSE} = \sqrt{\frac{1}{QP} \sum_{q=1}^Q \|\hat{\boldsymbol{\xi}}_q - \boldsymbol{\xi}_q\|_2^2} \quad (38)$$

where $\hat{\boldsymbol{\xi}}_q$ ($\hat{\boldsymbol{\xi}}_q \in \mathbb{C}^{P \times 1}$) is the estimation of $\boldsymbol{\xi}_q$ in the q -th simulation, P is the number of parameters, Q is the number of independent simulations and $\|\cdot\|_2$ denotes the ℓ_2 norm.

In the simulations, the direction grid of MSBL-IRLS is from -60° to 60° with 1° intervals. In implementing Algorithm 2, we set $\delta = 3^\circ$, $\varepsilon_1 = 0.005^\circ$ and $\iota = 10$. Each statistical result is an average over 1000 independent runs. The source signals are uncorrelated Gaussian processes with identical power, and the

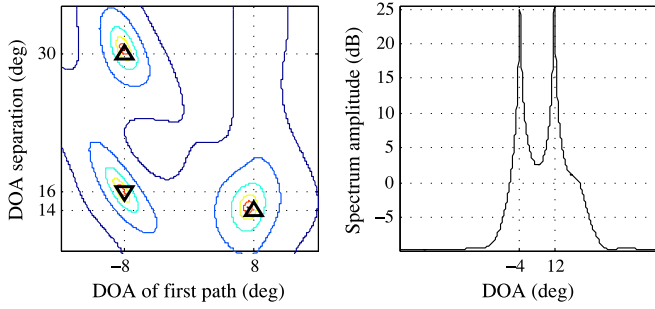


Fig. 1. Left: contour plot of 2-D spatial spectrum, those points of true DOA groups are marked by ‘ \triangle ’, the type II ambiguous point is marked by ‘ ∇ ’. Right: 1-D spatial spectrum.

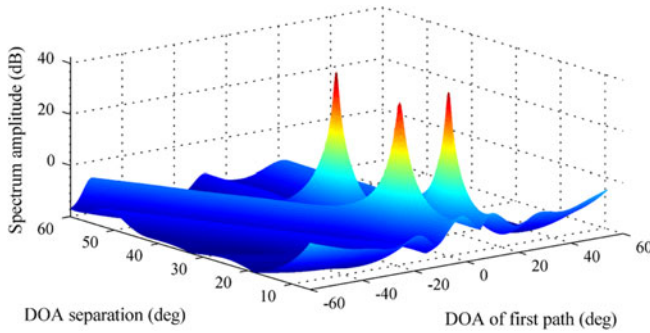


Fig. 2. 2-D spatial spectrum.

SNR is defined as $10 \log_{10}(\sigma_s^2/\sigma_n^2)$, where $\sigma_s^2 (= \sigma_1^2 = \dots = \sigma_K^2)$ is the power of the direct signals. Two array geometries are considered, a 10-element ULA with a half wavelength element spacing, and a 10-element nonuniform linear array (NLA) in which the locations of these sensors are $0\chi, 1\chi, 2\chi, 4\chi, 5\chi, 6\chi, 7\chi, 9\chi, 10\chi$ and 11χ with χ denoting the half wavelength. In the following experiments, unless otherwise noted, the ULA is used. Note that, among the compared algorithms, only Zhang’s method [26] and our algorithms exploit the SA information, but Zhang’s method only applies to ULA.

A. Spatial Spectrum of Function J_1

Since J_1 is an extended cost function of the standard MUSIC, naturally, we use k -D spatial spectrum to denote the k -D space of J_1 in the following. In the first experiment, in order to visualize the spatial spectrum, the maximum path number of sources is set to 2. Consider four sources ($K = 4$) that undergo multipath propagation impinging on the array. We set $\theta_1 = -4^\circ$, $\theta_2 = 12^\circ$, $\theta_3 = [-8^\circ, 22^\circ]^T$, $\theta_4 = [8^\circ, 22^\circ]^T$, $\bar{c}_3 = 0.89 \exp(j1.08\pi)$, $\bar{c}_4 = 0.63 \exp(j0.75\pi)$, $T = 200$ and SNR = 10 dB.

By R4, the 1-D spatial spectrum does not contain any ambiguity, which is verified by the simulation as shown in the right figure of Fig. 1. Obviously, the 1-D spatial spectrum only has strong peaks around the true DOA groups $\{-4^\circ\}$ and $\{-12^\circ\}$. However, the 2-D spatial spectrum contains both the type I and type II ambiguities. Through the guide lines of algorithm 3, we can easily depress the type I ambiguities by eliminating the contribution of the signals coming from $\{-4^\circ\}$ and $\{-12^\circ\}$ in the array covariance matrix. The 2-D spatial spectrum is shown in Fig. 2 and the left figure of Fig. 1. In order to fulfill the condi-

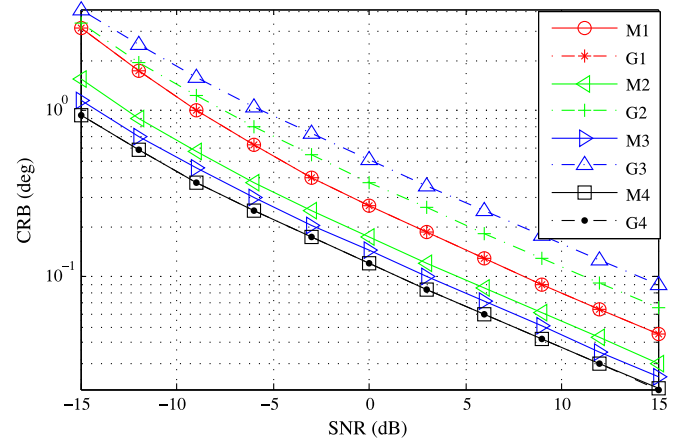


Fig. 3. CRB comparison: MCRB and GCRB versus SNR. M_k and G_k denote the MCRB and GCRB of scenario k ($k = 1, 2, 3, 4$), respectively.

tion of the searching area as discussed after (9), we search the DOA of the first path and the separation between two DOAs in obtaining the 2-D spatial spectrum. Then the coordinate values corresponding to these true groups and the type II ambiguous group respectively are $\{-8, 30\}$, $\{8, 14\}$ and $\{-8, 16\}$, which indeed are the strong peaks as shown in the figures. Furthermore, the values of these peaks are much larger than 0 dB, namely substituting the vector corresponding to any one of these peaks to the function J_2 (the inverse of J_1) would result in a very small value, which provide an intuitive understanding of the effectiveness of the thresholding method in Algorithm 3.

B. Comparison between MCRB and GCRB

In the second experiment, we compare the MCRB and GCRB in the following four scenarios.

- 1) $K = 6$, $\{P_k = 1\}_{k=1}^6$, namely, all the six equal-power signals are uncorrelated and arrive from $-30^\circ, -20^\circ, -10^\circ, 10^\circ, 20^\circ$ and 30° , respectively.
- 2) $K = 3$, $\{P_k = 2\}_{k=1}^3$. The DOA groups are $\{-30^\circ, 10^\circ\}$, $\{-20^\circ, 20^\circ\}$ and $\{-10^\circ, 30^\circ\}$, the corresponding FCs are $\{1, \exp(j0.22\pi)\}$, $\{1, \exp(j1.17\pi)\}$ and $\{1, \exp(j1.63\pi)\}$, respectively.
- 3) $K = 2$, $\{P_k = 3\}_{k=1}^2$. The DOA groups are $\{-30^\circ, -10^\circ, 20^\circ\}$ and $\{-20^\circ, 10^\circ, 30^\circ\}$, the corresponding FCs are $\{1, \exp(j0.81\pi), \exp(j0.19\pi)\}$ and $\{1, \exp(j1.92\pi), \exp(j1.17\pi)\}$, respectively.
- 4) $K = 1$, $P_1 = 3$, The DOAs are $-30^\circ, -10^\circ$ and 20° , the corresponding FCs are $1, \exp(j0.17\pi)$ and $\exp(j1.80\pi)$, respectively.

In this experiment, we set $T = 200$, and the SNR is varied from -15 dB to 15 dB. The CRBs for these four conditions are plotted in Fig. 3, which shows the following four results.

- 1) Both the MCRB and GCRB decrease monotonically as the SNR increases.
- 2) Both the MCRB and GCRB decrease as the total number of sources decreases.
- 3) In scenarios 2) and 3), MCRB is significantly lower than GCRB, while in the other two cases the two CRBs are identical.

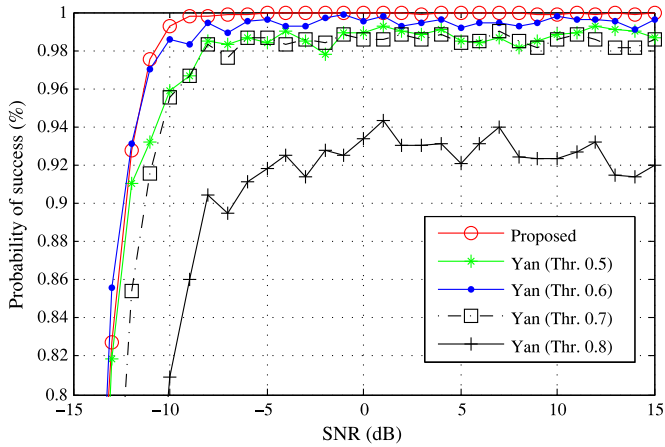


Fig. 4. Estimation performance of SA estimation: probability of successful SA estimation versus SNR.

- 4) The GCRB in the scenario where some of the incident signals are coherent is greater than that in the scenario where all the incident signals are uncorrelated. However, the effect of signal coherency on MCRB is contrary to that on the GCRB.

C. Performance Investigation for Well Separated DOAs

In the following two experiments, we study the estimation performance for the well separated case, and we consider three far-field sources impinging on the array through multiple paths, where the direct signals arrive from $-17^\circ + a_1$, $-8^\circ + a_2$ and $4^\circ + a_3$, respectively, the indirect signals of the first source and the second source respectively arrive from $13^\circ + a_4$ and $25^\circ + a_5$, and the corresponding FCs are fixed to $0.7 \exp(j1.4\pi)$ and $0.8 \exp(j0.7\pi)$, respectively. In each trail, $\{a_k\}_{k=1}^5$ are randomly chosen from -0.5° to 0.5° . The number of snapshots T is fixed to 200. For the scenario described above, we have $K = 3$, $K_D = K_S = 5$ and $K_D - K + 1 = 3$. As discussed in section IV-A, there are two possible combinations of (P_1, P_2, P_3) , which are $(1, 1, 3)$ and $(1, 2, 2)$.

The third experiment illustrates the probability of successful SA estimation for the well separated case. The proposed SA estimation algorithm, i.e., Algorithm 1, is compared with the Yan's method [27] with different threshold values. The errors of coarse DOA estimates are generated by drawing samples from a Gaussian process with mean zero and covariance 1.5° , and the generated errors are limited in the range of $[-4^\circ, 4^\circ]$ to make sure a meaningful definition of the SA set. The SNR is varied from -15 dB to 15 dB. The results are shown in Fig. 4. It can be seen that the proposed method can achieve a 100% success rate when $\text{SNR} \geq -5$ dB and has better performance than Yan's method. Yan's method cannot achieve a 100% success rate even at high SNRs (using the optimal threshold value 0.6).

The fourth experiment investigates the DOA and FCs estimation performance of the new methods, in comparison with the stochastic (unconditional) maximum likelihood estimator (UMLE, [34]), FBSS-based ESPRIT [5], EPUMA [25], MODE [23] and Zhang's method [26]. The SNR is varied from -10 dB to 20 dB. The statistical results are shown in Fig. 5 and Fig. 6.

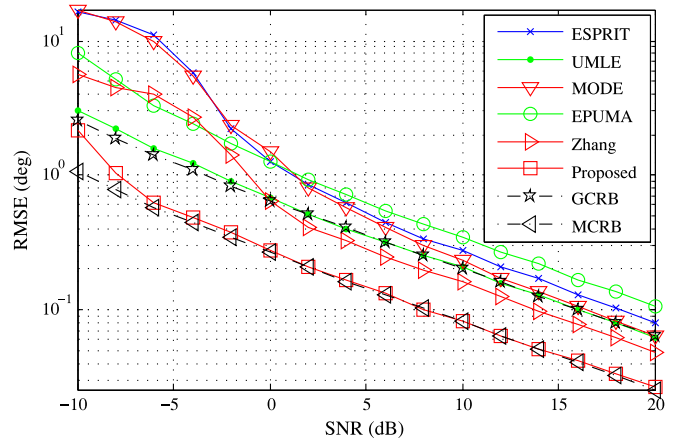


Fig. 5. DOA RMSE versus SNR when all the signals are well separated.

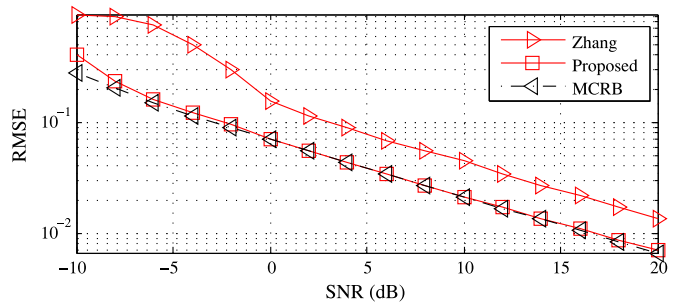


Fig. 6. FC RMSE versus SNR when all the signals are well separated.

In implementing the proposed algorithm the SA is estimated by Algorithm 1, while in implementing Zhang's method the true SA information is used.

The results show that the proposed method gives the best performance and significantly outperforms the other algorithms. The RMSE of the DOA and FCs estimation of the proposed method can closely approach the corresponding MCRB when the SNR is greater than -5 dB. Compared with the traditional methods which do not exploit the coherency structure information, Zhang's method improves the estimation accuracy a lot and can even beat the GCRB when $\text{SNR} > 0$ dB. Since Zhang's method is based on the FBSS approach which reduces the effective array aperture, there is a considerable gap between it and the proposed method.

D. Performance Investigation in a Generalized Case

In this subsection, we consider a case that $K'_D < K_D < K_S$. We design three experiments to investigate the effectiveness of algorithm 3 in coping with this case. The fifth experiment illustrates the feasibility of hard thresholding DOA group detection. The sixth and seventh experiments investigate the performance of the DOA and FCs estimation of Algorithm 3 versus SNR and the number snapshots, respectively.

For these three experiments, we consider three sources through multiple paths impinging on the array, the directions of the direct signals are $-37^\circ + b_1$, $-20^\circ + b_2$ and $-8^\circ + b_3$. Meanwhile, the directions of the indirect signals are $10^\circ + b_4$, $\{10^\circ + b_4, 23^\circ + b_5\}$ and $10.1^\circ + b_4$, the corresponding FCs are

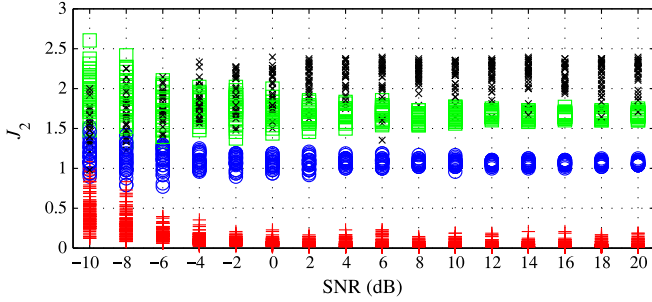


Fig. 7. Feasibility of hard thresholding DOA group detection: J_2 of those true DOA groups and type II ambiguities are marked as '+', the minimum J_2 of the rest groups with $\theta \in \mathbb{R}^{1 \times 1}$, $\theta \in \mathbb{R}^{2 \times 1}$ and $\theta \in \mathbb{R}^{3 \times 1}$ are marked as '□', '○' and '×', respectively.

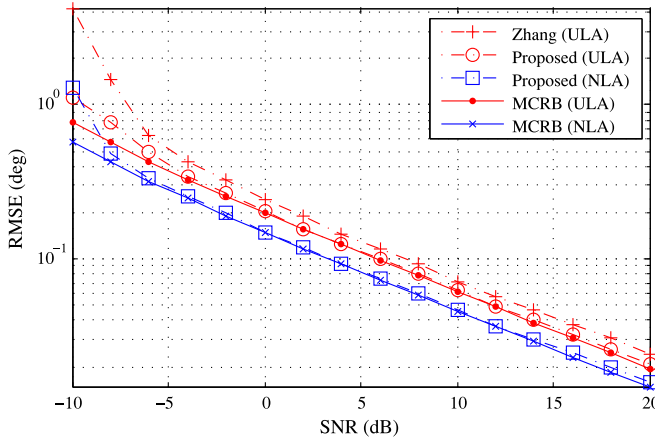


Fig. 8. DOA RMSE versus SNR for a generalized case.

$0.71 \exp(j0.24\pi)$, $\{0.72 \exp(j0.78\pi), 0.78 \exp(j0.89\pi)\}$ and $0.82 \exp(j1.29\pi)$, respectively. In each trial, $\{b_k\}_{k=1}^5$ are randomly chosen from -0.5° to 0.5° . In implementing Algorithm 3, the hard thresholding parameter ε_2 is set to 0.6.

In the fifth experiment, the error of each DOA in the coarse DOA estimation is randomly chosen from -0.5° to 0.5° for each trial. The number of snapshots T is fixed to 200, and the SNR is varied from -10 dB to 20 dB. As discussed in Section IV, only the true DOA groups and the DOA groups of the type II ambiguities would result in $J_2(\theta, \mathbf{U}_N^k) \rightarrow 0$ ($\theta \in \mathbb{R}^{k \times 1}$, $k = 1, 2, 3$). Then, we plot J_2 of these DOA groups and the minimum J_2 of the others in each trial. Thirty independent trials are done for each SNR, and the results are shown in Fig. 7, which shows that the two groups of data are well separated when SNR is greater than -6 dB.

In both the sixth and seventh experiments, the proposed algorithm is compared with the Zhang's method and the MCRB. Note that, in the considered condition with nearly overlapped incident signals, to the best of our knowledge, only the Zhang's method is capable of resolving all the DOAs. Moreover, the proposed algorithm applies to arbitrary array. Hence, the performance of the proposed algorithm and the corresponding MCRB for the NLA introduced at the beginning of this section are also presented.

Fig. 8 and Fig. 9 present the DOA and FCs estimation performance versus SNR with $T = 200$, respectively. Since when a wrong SA is obtained, we cannot calculate the correspond-

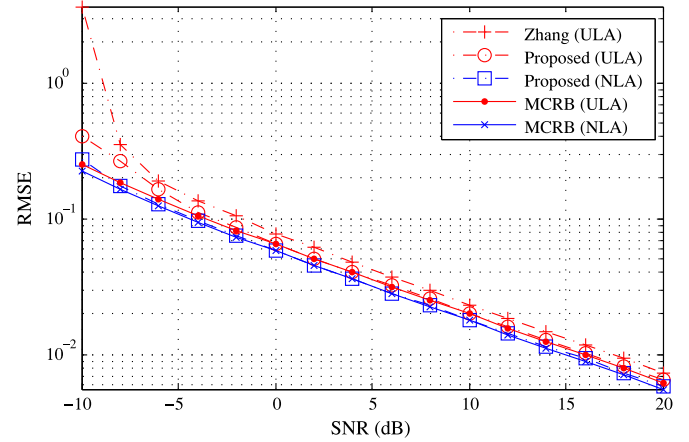


Fig. 9. FC RMSE versus SNR for a generalized case.

TABLE I
THE PROBABILITIES OF SUCCESSFUL SA ESTIMATION IN THE SIXTH AND SEVENTH EXPERIMENTS

SNR (dB)	-10	-8	-6	-4 ~ 15
Prob. (ULA, %)	68.2	97.6	99.9	100
Prob. (NLA, %)	68.2	97.0	99.9	100

Snapshots	20	40	60	80	100 ~ 200
Prob. (ULA, %)	64.6	93.9	99.1	99.9	100
Prob. (NLA, %)	65.2	94.0	99.3	100	100

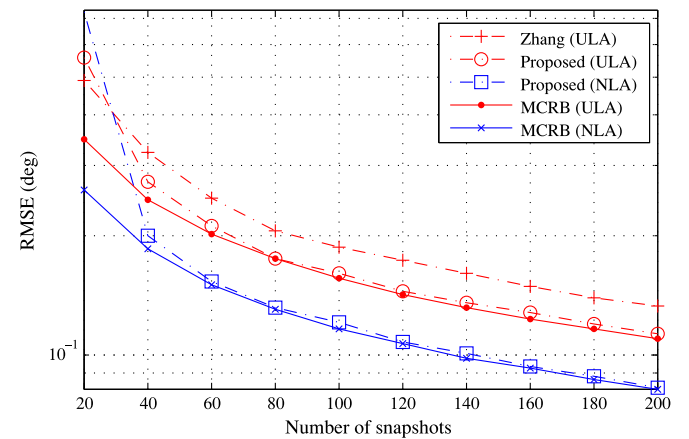


Fig. 10. DOA RMSE versus the number of snapshots for a generalized case.

ing RMSEs of DOA and FCs estimation, only the trials with successful SA estimation are used to calculate all the RMSEs. The probabilities of successful SA estimation for each SNR are shown in Table I, which is consistent with the result in Fig. 7. Fig. 8 and Fig. 9 demonstrate that the proposed algorithm outperforms the Zhang's method in both DOA and FCs estimation, and its RMSE curves can closely approach the corresponding CRBs when SNR is greater than -5 dB. It is also shown that the proposed algorithm works well when using the NLA, and a significant gain can be achieved in comparison with using the ULA, where these two arrays have an identical number of sensors but the NLA has a larger array aperture.

Fig. 10 shows the statistical results of DOA estimation versus the number of snapshots with SNR = 5 dB. As same as in the previous experiment, only the trials with successful SA

estimation are used to calculate the RMSE. The probabilities of successful SA estimation for different snapshot numbers are shown in Table I. It is shown that Algorithm 3 can achieve a 100% success rate when the number of snapshots is greater than 80 in both the array geometry conditions. Moreover, it can be clearly seen from Fig. 10 that, the proposed method outperforms Zhang's method and can closely approach the MCRB when the number of snapshots is greater than 60.

VII. CONCLUSION

Effective SA, DOA and FCs estimation methods have been proposed in this paper for multipath signals. These methods are based on a rank reduction property for multipath signal model under the existence of multiple groups of coherent signals. Further, the closed-form stochastic Cramér-Rao bound for DOA and FCs estimation of multipath model exploiting the multipath structure information has been provided. Unlike traditional subspace based DOA estimators for coherent signals, the new approaches are applicable to arbitrary array geometry while without decreasing the effective array aperture. More importantly, by exploiting the multipath structure information, the proposed DOA estimation methods can achieve significantly improved performance over traditional methods. Simulation results have verified the effectiveness of the new methods.

APPENDIX A PROOF OF R1

Define $\varphi_1 = [\theta_{11}, \theta_{21}, \dots, \theta_{K1}]^T$ consisting of all the DOAs of direct signals and $\varphi_0 \in \mathbb{R}^{(K_D - K) \times 1}$ consisting of all the distinct DOAs of indirect signals. Then the virtual steering vectors can be rewritten as

$$\mathbf{b}_k = \mathbf{a}(\theta_{k1}) + \mathbf{A}(\varphi_0) \tilde{\mathbf{c}}'_k, k = 1, 2, \dots, K, \quad (39)$$

where $\tilde{\mathbf{c}}'_k \in \mathbb{C}^{(K_D - K) \times 1}$ is an augmented FC vector consisting of $P_k - 1$ nonzero elements $c_{k2}, c_{k3}, \dots, c_{kP_k}$. Using the above definitions, \mathbf{B} can be rewritten as

$$\mathbf{B} = \mathbf{A}(\boldsymbol{\eta}_\theta) \mathbf{C} = [\mathbf{A}(\varphi_1), \mathbf{A}(\varphi_0)] \begin{bmatrix} \mathbf{I}_K \\ \mathbf{C}' \end{bmatrix} \quad (40)$$

with $\mathbf{C}' = [\tilde{\mathbf{c}}'_1, \tilde{\mathbf{c}}'_2, \dots, \tilde{\mathbf{c}}'_K]$. From (40), it is clear that when $K_D \leq M$, $[\mathbf{A}(\varphi_1), \mathbf{A}(\varphi_0)]$ is of full column rank, and then we get

$$\begin{aligned} K &\geq \text{rank}(\mathbf{B}) \\ &\geq \text{rank}([\mathbf{A}(\varphi_1), \mathbf{A}(\varphi_0)]) + \text{rank} \left(\begin{bmatrix} \mathbf{I}_K \\ \mathbf{C}' \end{bmatrix} \right) - K_D \\ &= K_D + K - K_D = K, \end{aligned} \quad (41)$$

which completes the proof of R1.

APPENDIX B PROOF OF R2

Since $\mathbf{U}_N^H \mathbf{A}(\boldsymbol{\theta}_k) \mathbf{c}_k = \mathbf{0}$ and $P_k \leq M - K$, it follows that $\text{rank}(\mathbf{U}_N^H \mathbf{A}(\boldsymbol{\theta}_k)) \leq P_k - 1$. Assume that $\text{rank}(\mathbf{U}_N^H \mathbf{A}(\boldsymbol{\theta}_k)) < P_k - 1$ holds. There must exist a $P_k \times 1$ nonzero vector

\mathbf{c}'_k ($\mathbf{c}'_k \not\parallel \mathbf{c}_k$) such that $\mathbf{U}_N^H \mathbf{A}(\boldsymbol{\theta}_k) \mathbf{c}'_k = \mathbf{0}$. By R1, we have $\text{null}(\mathbf{U}_N^H) = \text{span}(\mathbf{B})$, which implies that $\mathbf{A}(\boldsymbol{\theta}_k) \mathbf{c}'_k \in \text{span}(\mathbf{B})$. Hence, there must exist a $K \times 1$ nonzero vector $\boldsymbol{\alpha}$ such that

$$\mathbf{B} \boldsymbol{\alpha} - \mathbf{A}(\boldsymbol{\theta}_k) \mathbf{c}'_k = [\mathbf{A}(\varphi_1), \mathbf{A}(\varphi_0)] \begin{bmatrix} \boldsymbol{\alpha}' \\ \mathbf{C}'' \boldsymbol{\alpha}'' \end{bmatrix} = \mathbf{0}, \quad (42)$$

where $\boldsymbol{\alpha}' = [\alpha_1, \dots, \alpha_{k-1}, \alpha_k - c'_{k1}, \alpha_{k+1}, \dots, \alpha_K]^T$, $\boldsymbol{\alpha}'' = [\alpha_1, \dots, \alpha_{k-1}, 1, \alpha_{k+1}, \dots, \alpha_K]^T$, φ_0 and φ_1 are defined in Appendix A, and \mathbf{C}'' is equal to \mathbf{C}' (defined in (40)) except for the k -th column, the nonzero elements of which are $\alpha_k c_{kp} - c'_{kp}$, $p = 2, 3, \dots, P_k$ with α_k and c'_{kp} denoting the k -th element of $\boldsymbol{\alpha}$ and p -th element of \mathbf{c}'_k , respectively. When $K_D \leq M$, the matrix $[\mathbf{A}(\varphi_1), \mathbf{A}(\varphi_0)]$ is of full column rank. Thus, it follows from (42) that $\boldsymbol{\alpha}' = \mathbf{0}$ and $\mathbf{C}'' \boldsymbol{\alpha}'' = \mathbf{0}$, which result in $\mathbf{c}'_k = \alpha_k \mathbf{c}_k$. This leads to a contradiction with the assumption, which completes the proof of R2.

APPENDIX C PROOF OF R3

Assume $\boldsymbol{\varphi} = \boldsymbol{\theta}_k + \Delta\boldsymbol{\varphi}$ with $\Delta\boldsymbol{\varphi} \neq \mathbf{0}$ and $|\Delta\varphi_p| \leq \kappa$, $p = 1, 2, \dots, P_k$, where $\Delta\varphi_p$ is the p -th element of $\Delta\boldsymbol{\varphi}$ and κ is a small real number such that $\varphi_p \notin \{\theta_{nq}; (n, q) \neq (k, p)\}_{n, q}$ ($p \in \{1, 2, \dots, P_k\}$) with φ_p denoting the p -th element of $\boldsymbol{\varphi}$. Since $P_k \leq M - K$, to prove R3, it suffices to prove that $\mathbf{U}_N^H \mathbf{A}(\boldsymbol{\varphi}) \in \mathbb{C}^{(M-K) \times P_k}$ is a full column rank matrix for arbitrary $\Delta\boldsymbol{\varphi} \neq \mathbf{0}$. This condition implies that the solution of $\mathbf{U}_N^H \mathbf{A}(\boldsymbol{\varphi}) \boldsymbol{\beta} = \mathbf{0}$ is $\boldsymbol{\beta} = \mathbf{0}$. Since $\text{span}(\mathbf{B}) = \text{null}(\mathbf{U}_N^H)$, for a given $\Delta\boldsymbol{\varphi}$ ($\Delta\boldsymbol{\varphi} \neq \mathbf{0}$) and arbitrary $\boldsymbol{\beta} \in \mathbb{C}^{K \times 1}$, $\mathbf{A}(\boldsymbol{\varphi}) \boldsymbol{\beta} \notin \text{span}(\mathbf{B})$ needs to be hold, or equivalently, the solution of

$$\mathbf{A}(\boldsymbol{\varphi}) \boldsymbol{\beta} + \mathbf{B} \boldsymbol{\alpha} = \mathbf{0} \quad (43)$$

is $\boldsymbol{\alpha} = \mathbf{0}$ and $\boldsymbol{\beta} = \mathbf{0}$. Indeed, when all the entries of $\Delta\boldsymbol{\varphi}$ are nonzero and $K_D + P_k \leq M$, by R1, $[\mathbf{A}(\boldsymbol{\varphi}), \mathbf{B}]$ is of full column rank, which implies that (43) only has zero solution.

When l ($l \in \{1, 2, \dots, P_k - 1\}$) entries of $\Delta\boldsymbol{\varphi}$ are zero, assuming that the corresponding indexes is contained in the set Υ and the complementary set is Υ^C , we can rewrite (43) as

$$\mathbf{A}(\varphi_{\Upsilon^C}) \boldsymbol{\beta}_{\Upsilon^C} + \mathbf{A}(\varphi_{\Upsilon}) \boldsymbol{\beta}_{\Upsilon} + \mathbf{A}(\boldsymbol{\eta}_\theta) \mathbf{C} \boldsymbol{\alpha} = \mathbf{0}, \quad (44)$$

where φ_{Υ} denotes the subvector formed with the elements of $\boldsymbol{\varphi}$ indexed by Υ . Similar to (40), (44) can be rewritten as

$$\mathbf{A}(\varphi_{\Upsilon^C}) \boldsymbol{\beta}_{\Upsilon^C} + [\mathbf{A}(\varphi_1), \mathbf{A}(\varphi_0)] \begin{bmatrix} \boldsymbol{\alpha} + \boldsymbol{\beta}_1 \\ \mathbf{C}' \boldsymbol{\alpha} + \boldsymbol{\beta}_0 \end{bmatrix} = \mathbf{0}, \quad (45)$$

where \mathbf{C}' , φ_1 and φ_0 are defined in Appendix A. When $\Delta\varphi_1 \neq 0$, we have that $\boldsymbol{\beta}_1 = \mathbf{0} \in \mathbb{R}^{K \times 1}$, and $\boldsymbol{\beta}_0 \in \mathbb{C}^{(K_D - K) \times 1}$ is obtained by augmenting $\boldsymbol{\beta}_{\Upsilon}$ with zeros. When $\Delta\varphi_1 = 0$, we have that the elements of $\boldsymbol{\beta}_1$ are zero except that its k -th element equals to the first element of $\boldsymbol{\beta}_{\Upsilon}$, i.e., β_1 , and $\boldsymbol{\beta}_0$ is obtained by augmenting the vector containing the last $l - 1$ elements of $\boldsymbol{\beta}_{\Upsilon}$ with zeros. Since $K_D + P_k \leq M$, the matrix $[\mathbf{A}(\varphi_{\Upsilon^C}), \mathbf{A}(\varphi_1), \mathbf{A}(\varphi_0)]$ is of full column rank, it follows from (45) that $\boldsymbol{\beta}_{\Upsilon^C} = \mathbf{0}$ and

$$\boldsymbol{\alpha} + \boldsymbol{\beta}_1 = \mathbf{0}, \quad (46)$$

$$\mathbf{C}' \boldsymbol{\alpha} + \boldsymbol{\beta}_0 = \mathbf{0}. \quad (47)$$

Clearly, when $\Delta\varphi_1 \neq 0$, it follows that $\alpha = \mathbf{0}$ and $\beta = \mathbf{0}$. When $\Delta\varphi_1 = 0$, from (46), we have $\{\alpha_q = 0\}_{q \neq k}$ and $\alpha_k = \beta_1$. However, $\bar{\mathbf{c}}'_k$ has $P_k - 1$ nonzero elements but β_0 has at most $l - 1$ nonzero elements, thus we still have $\alpha = \mathbf{0}$ and $\beta = \mathbf{0}$. The proof is finished.

APPENDIX D PROOF OF R4

For a given $\theta \in \mathbb{R}^{i \times 1}$, if $[\mathbf{A}(\theta), \mathbf{B}]$ is of full column rank, it is easy to verify that $\mathbf{U}_N^H \mathbf{A}(\theta) \alpha \neq \mathbf{0}$ holds for arbitrary nonzero vector $\alpha \in \mathbb{C}^{i \times 1}$, which means that the given θ is not an ambiguous point. When $i = 1$ and $K_D + i \leq M$, by R1, we have that the matrix $[\mathbf{a}(\theta), \mathbf{B}]$ is of full column rank for any $\theta \notin \{\theta_{kp}\}$. Hence, there is no ambiguity. When $i > 1$, $K_D + i \leq M$ and any entries of θ is not contained in η_θ , by R1, we still have that $[\mathbf{A}(\theta), \mathbf{B}]$ is a full column rank matrix, and then there is no ambiguity. Thus, we only need to consider the scenario that $i > 1$ and at least one entry of θ is contained in η_θ .

Assume that θ and φ_p ($p \in \{0, 1\}$) have γ_p common elements, where φ_0 and φ_1 are defined in Appendix A. According to the correspondence between θ and φ_p ($p \in \{0, 1\}$), $\mathbf{A}(\theta)$ can be partitioned into three submatrices $\mathbf{A}_0 \in \mathbb{C}^{M \times \gamma_0}$, $\mathbf{A}_1 \in \mathbb{C}^{M \times \gamma_1}$ and $\mathbf{A}_2 \in \mathbb{C}^{M \times (i - \gamma_0 - \gamma_1)}$. If ambiguity exists, there must exist an $i \times 1$ nonzero vector $\alpha = [\alpha_0^T, \alpha_1^T, \alpha_2^T]^T$ ($\alpha_0 \in \mathbb{C}^{\gamma_0 \times 1}$, $\alpha_1 \in \mathbb{C}^{\gamma_1 \times 1}$, $\alpha_2 \in \mathbb{C}^{(i - \gamma_0 - \gamma_1) \times 1}$), such that the equation

$$[\mathbf{B}, \mathbf{A}_0, \mathbf{A}_1, \mathbf{A}_2] \begin{bmatrix} \beta \\ \alpha \end{bmatrix} = \mathbf{0} \quad (48)$$

has nonzero solution $\beta \in \mathbb{C}^{K \times 1}$. We can merge \mathbf{A}_0 and \mathbf{A}_1 into \mathbf{B} (note that $\mathbf{B} = \mathbf{A}(\varphi_1) + \mathbf{A}(\varphi_0)\mathbf{C}'$, see (40)). Assume that $\mathbf{A}'(\varphi_0)$ and $\mathbf{A}'(\varphi_1)$ are the column rearranged matrices of $\mathbf{A}(\varphi_0)$ and $\mathbf{A}(\varphi_1)$, respectively, such that we have

$$[\mathbf{A}'(\varphi_0), \mathbf{A}'(\varphi_1), \mathbf{A}_2] \begin{bmatrix} \bar{\mathbf{C}}' \beta' + \alpha'_0 \\ \beta' + \alpha'_1 \\ \alpha_2 \end{bmatrix} = \mathbf{0}, \quad (49)$$

with $\alpha'_0 = [\alpha_0^T, \mathbf{0}^T]^T$, $\alpha'_1 = [\alpha_1^T, \mathbf{0}^T]^T$. In order to make sure the consistency between (48) and (49), $\bar{\mathbf{C}}'$ is obtained by rearranging both the row sequence (according to the rearrangement from $\mathbf{A}(\varphi_0)$ to $\mathbf{A}'(\varphi_0)$) and column sequence (according to the rearrangement from $\mathbf{A}(\varphi_1)$ to $\mathbf{A}'(\varphi_1)$) of \mathbf{C}' , and β' is a rearranged vector of β (according to the rearrangement from $\mathbf{A}(\varphi_1)$ to $\mathbf{A}'(\varphi_1)$). Clearly, the matrix $[\mathbf{A}'(\varphi_0), \mathbf{A}'(\varphi_1), \mathbf{A}_2] \in \mathbb{C}^{M \times (K_D + i - \gamma_0 - \gamma_1)}$ is of full column rank when $K_D + i - \gamma_0 - \gamma_1 < K_D + i \leq M$. Thus, the solution of (49) is given by

$$\begin{cases} \bar{\mathbf{C}}' \beta' + \alpha'_0 = \mathbf{0} \\ \beta' + \alpha'_1 = \mathbf{0} \\ \alpha_2 = \mathbf{0} \end{cases}. \quad (50)$$

It follows that

$$\bar{\mathbf{C}}'_{\gamma_1} \alpha_1 = \alpha'_0, \quad (51)$$

where $\bar{\mathbf{C}}'_{\gamma_1}$ is the matrix consisting of the first γ_1 column of $\bar{\mathbf{C}}'$. Since $\beta' = -\alpha'_1$, we only need to prove that there exist nonzero vectors α_0 and α_1 such that (51) holds. When $\gamma_1 = 0$, it follows from (51) that $\alpha = \mathbf{0}$. When $\gamma_1 \geq 1$, the number of minimum nonzero rows of $\bar{\mathbf{C}}'_{\gamma_1}$ is $i - 1$, and in (51), maximum $\gamma_1 - 1$ nonzero rows can be eliminated by using α_1 . Hence, the minimum number of nonzero elements in α'_0 needs to satisfy $\gamma_0 \geq i - 1 - (\gamma_1 - 1)$. By definition, we also have $\gamma_0 + \gamma_1 \leq i$, which implies that $\gamma_0 + \gamma_1 = i$ and the number of the nonzero rows of $\bar{\mathbf{C}}'_{\gamma_1}$ needs to be $i - 1$, otherwise, (51) would not hold for any $\alpha \neq \mathbf{0}$. Since one column of $\bar{\mathbf{C}}'$ corresponds to one source and the rows of $\bar{\mathbf{C}}'$ correspond to distinct DOAs, it follows that, if there exist i' sources having i paths and identical indirect paths, there must exist nonzero vector α such that (48) has nonzero solution β . From the above analysis, any DOA vector consisting of any i distinct DOAs of these i' sources satisfies that (48) exists nonzero solution. That is, there are $C_{i'+i-1}^i - i'$ ambiguous points brought by these i' sources. The proof is finished.

APPENDIX E PROOF OF (12)

It can be easily verified that $J_2(\theta, \mathbf{U}_N) \geq 0$. Hence, to prove (12), it is enough to show that at least one wrong DOA group satisfies $J_2(\theta, \mathbf{U}_N) > 0$. By R4, there could only exist type I ambiguous points for the well separated case. Meanwhile, at least one of the wrong DOA groups in S_w is not type I ambiguous point. Therefore, to prove (12), it suffices to show that the vector $\theta_w \in \mathbb{R}^{P_q \times 1}$ ($q \in \{1, 2, \dots, K\}$) consisting of the subvectors of $\theta_1, \theta_2, \dots, \theta_K$ satisfies $\det(\mathbf{A}^H(\theta_w) \mathbf{U}_N \mathbf{U}_N^H \mathbf{A}(\theta_w)) > 0$, or equivalently, the matrix $[\mathbf{B}, \mathbf{A}(\theta_w)]$ is of full column rank.

Let $\theta_w = [\theta_1^{sT}, \theta_2^{sT}, \dots, \theta_K^{sT}]^T$, where $\theta_k^s \in \mathbb{R}^{P_k^s}$ is a subvector of θ_k , $P_k^s < P_k$ and $P_1^s + P_2^s + \dots + P_K^s = P_q$. Assume that the matrix $[\mathbf{B}, \mathbf{A}(\theta_w)]$ is not of full column rank. There must exist nonzero vector $\alpha = [\alpha_0^T, \beta^T]^T$ with $\beta = [\alpha_1^T, \alpha_2^T, \dots, \alpha_K^T]^T$, $\alpha_0 \in \mathbb{C}^{K \times 1}$ and $\alpha_k \in \mathbb{C}^{P_k^s \times 1}$ such that

$$\mathbf{B} \alpha_0 + \mathbf{A}(\theta_w) \beta = \mathbf{0}. \quad (52)$$

Without loss of generality, assume that θ_k^s is formed with the first P_k^s elements of θ_k . We can augment α_k^s to $\alpha_k^a = [\alpha_k^{sT}, \mathbf{0}^T]^T$, where $\mathbf{0}$ denotes the $(P_k - P_k^s) \times 1$ vector of 0s. And then (52) can be rewritten as

$$\mathbf{A}(\eta_\theta)(\mathbf{C} \alpha_0 + \beta^a) = \mathbf{0}, \quad (53)$$

where $\beta^a = [\alpha_1^{aT}, \alpha_2^{aT}, \dots, \alpha_K^{aT}]^T$. When $K_D + P_K \leq M$, (53) implies that $\mathbf{C} \alpha_0 + \beta^a = \mathbf{0}$, or equivalently,

$$\alpha_{0k} \mathbf{c}_k + \alpha_k^a = \mathbf{0}, k = 1, 2, \dots, K, \quad (54)$$

where α_{0k} is the k -th element of α_0 . Since α_k^a has at most P_k^s nonzero elements and $P_k^s < P_k$, it follows that $\alpha = \mathbf{0}$, which completes the proof.

APPENDIX F PROOF OF R5

Let $\{\bar{\mathbf{b}}_l\}_{l=1}^{D'_p}$ and $\{\bar{\sigma}_l^2\}_{l=1}^{D'_p}$ denote the virtual steering vectors and signal powers estimated from the DOA groups in S' ,

respectively. By R4, when there exist ambiguities, we have that $D_p \geq 2$ and $p \geq 2$. Thus, we only need to consider the scenario that $D_p \geq 2$ and $p \geq 2$. Without loss of generality, assume that the first D_p elements of S' are the true DOA groups, the rest groups in S' are the type II ambiguities. We also assume that all the parameters are perfectly estimated. Then we have

$$\mathbf{R}_p = \sum_{l=1}^{D_p} \bar{\sigma}_l^2 \bar{\mathbf{b}}_l \bar{\mathbf{b}}_l^H = \mathbf{B}_p \boldsymbol{\Sigma}_p \mathbf{B}_p^H \quad (55)$$

where \mathbf{R}_p is defined in (15), $\mathbf{B}_p = [\bar{\mathbf{b}}_1, \bar{\mathbf{b}}_2, \dots, \bar{\mathbf{b}}_{D_p}]$ and $\boldsymbol{\Sigma}_p$ is a diagonal matrix with $\bar{\sigma}_1^2, \bar{\sigma}_2^2, \dots, \bar{\sigma}_{D_p}^2$ in its main diagonal.

From the proof of R4, we know that $\bar{\mathbf{b}}_l, l \in \{D_p + 1, D_p + 2, \dots, D'_p\}$ is a linear combination of the columns of \mathbf{B}_p , it can be expressed as

$$\bar{\mathbf{b}}_l = \mathbf{B}_p \boldsymbol{\beta}_l, \quad (56)$$

where $\boldsymbol{\beta}_l$ contains at least two nonzero elements. For $l \in \{1, 2, \dots, D_p\}$, $\bar{\mathbf{b}}_l$ has an unified expression as (56), but $\boldsymbol{\beta}_l$ is a unit vector with only one nonzero entry (its l -th element equals 1). It follows from (17) and (18) that the equality in (21) holds when the true DOA groups are selected. Suppose that D_p groups containing at least one ambiguity are selected from S' , and let

$$\mathbf{R}'_p = \sum_{l=1}^{D_p} \bar{\sigma}_{q_l}^2 \bar{\mathbf{b}}_{q_l} \bar{\mathbf{b}}_{q_l}^H = \mathbf{B}_p \boldsymbol{\Sigma}'_p \mathbf{B}_p^H, \quad (57)$$

where $\boldsymbol{\Sigma}'_p = \sum_{l=1}^{D_p} \bar{\sigma}_{q_l}^2 \boldsymbol{\beta}_{q_l} \boldsymbol{\beta}_{q_l}^H$ and q_1, q_2, \dots, q_{D_p} denote the indexes of the selected elements in S' . Obviously, $\boldsymbol{\Sigma}'_p$ is a non-diagonal matrix, and then we get $\boldsymbol{\Sigma}'_p \neq \boldsymbol{\Sigma}_p$. Moreover, we have

$$\begin{aligned} \mathbf{R}'_Y - \mathbf{R}'_p &= \mathbf{R}'_Y^{p+1} + \mathbf{R}_p - \mathbf{R}'_p \\ &= [\mathbf{B}_p, \mathbf{B}_{p+1}, \dots, \mathbf{B}_{P_K}] \bar{\boldsymbol{\Sigma}}_p [\mathbf{B}_p, \mathbf{B}_{p+1}, \dots, \mathbf{B}_{P_K}]^H, \end{aligned} \quad (58)$$

where $\bar{\boldsymbol{\Sigma}}_p = \text{blkdiag}(\boldsymbol{\Sigma}_p - \boldsymbol{\Sigma}'_p, \boldsymbol{\Sigma}_{p+1}, \dots, \boldsymbol{\Sigma}_{P_K})$. Based on the assumption that \mathbf{B} is of full column rank, it follows that

$$\text{rank}(\mathbf{R}'_Y - \mathbf{R}'_p) = \text{rank}(\bar{\boldsymbol{\Sigma}}_p) > K_{p+1},$$

which completes the proof of R5.

APPENDIX G PROOF OF R6

When $K = 1$, the MCRB shown in (31) can be directly simplified to

$$CRB^M(\boldsymbol{\eta}) = \frac{\sigma_n^2}{2Tu} \left\{ \Re \left\{ (\mathbf{H}^H P_{\mathbf{b}_1}^\perp \mathbf{H})^T \right\} \right\}^{-1} \quad (59)$$

where $u = \sigma_1^4 \mathbf{b}_1^H \mathbf{R}_Y^{-1} \mathbf{b}_1$. In order to extract the DOA block in $CRB^M(\boldsymbol{\eta})$, we rewrite (59) as

$$CRB^M(\boldsymbol{\eta}) = \frac{\sigma_n^2}{2Tu} \left\{ \Re \left\{ (\bar{\mathbf{H}}^H \bar{\mathbf{H}})^T \right\} \right\}^{-1}, \quad (60)$$

where $\bar{\mathbf{H}} = [P_{\mathbf{b}_1}^\perp \mathbf{H}_\theta, P_{\mathbf{b}_1}^\perp \mathbf{H}_{CR}, jP_{\mathbf{b}_1}^\perp \mathbf{H}_{CR}]$. Then the technique used for block-diagonalizing the Fisher matrix of the determined

model in [35] also applies to this problem. Define

$$\mathbf{F} = \begin{bmatrix} \mathbf{I}_{K_S} & \mathbf{0} & \mathbf{0} \\ -\Re(\mathbf{K}) & \mathbf{I}_{K_S-1} & \mathbf{0} \\ -\Im(\mathbf{K}) & \mathbf{0} & \mathbf{I}_{K_S-1} \end{bmatrix}, \quad (61)$$

where $\mathbf{K} = (\mathbf{H}_{CR}^H P_{\mathbf{b}_1}^\perp \mathbf{H}_{CR})^{-1} \mathbf{H}_{CR}^H P_{\mathbf{b}_1}^\perp \mathbf{H}_\theta$. Then we have

$$\bar{\mathbf{H}} \mathbf{F} = \left[P_{\mathbf{b}_1}^\perp \mathbf{H}_{CR}, P_{\mathbf{b}_1}^\perp \mathbf{H}_\theta, P_{\mathbf{b}_1}^\perp \mathbf{H}_{CR}, jP_{\mathbf{b}_1}^\perp \mathbf{H}_{CR} \right]. \quad (62)$$

Since \mathbf{F} is a real matrix, it can be verified that (only the DOA block is given, the blocks of no interest are denoted by ' \times ')

$$\begin{aligned} CRB^M(\boldsymbol{\eta}) &= \frac{\sigma_n^2}{2Tu} \mathbf{F} \left\{ \mathbf{F}^T \Re \left\{ (\bar{\mathbf{H}}^H \bar{\mathbf{H}})^T \right\} \mathbf{F} \right\}^{-1} \mathbf{F}^T \\ &= \frac{\sigma_n^2}{2Tu} \mathbf{F} \left\{ \Re \left\{ (\mathbf{F}^H \bar{\mathbf{H}}^H \bar{\mathbf{H}} \mathbf{F})^T \right\} \right\}^{-1} \mathbf{F}^T \\ &= \begin{bmatrix} CRB^M(\boldsymbol{\eta}_\theta) & \times & \times \\ \times & \times & \times \\ \times & \times & \times \end{bmatrix} \end{aligned} \quad (63)$$

with

$$CRB^M(\boldsymbol{\eta}_\theta) = \frac{\sigma_n^2}{2Tu} \left\{ \Re \left\{ (\mathbf{H}_\theta^H P_{\mathbf{b}_1}^\perp P_\Delta^\perp P_{\mathbf{b}_1}^\perp \mathbf{H}_\theta)^T \right\} \right\}^{-1} \quad (64)$$

where $\Delta = P_{\mathbf{b}_1}^\perp \mathbf{H}_{CR}$. Next, we show the equivalence between (34) and (64). As $\mathbf{b}_1 = \mathbf{A}(\boldsymbol{\eta}_\theta) \mathbf{c}_1$, and \mathbf{H}_{CR} is a submatrix of $\mathbf{A}(\boldsymbol{\eta}_\theta)$, we have

$$\begin{cases} \text{span}(P_{\mathbf{A}(\boldsymbol{\eta}_\theta)}^\perp) \subset \text{span}(P_{\mathbf{b}_1}^\perp) \\ \text{span}(P_{\mathbf{A}(\boldsymbol{\eta}_\theta)}^\perp) \subset \text{span}(P_\Delta^\perp) \end{cases}, \quad (65)$$

$\dim(P_{\mathbf{b}_1}^\perp) = 1$ and

$$\dim(P_{\mathbf{A}(\boldsymbol{\eta}_\theta)}^\perp) = M - K_S. \quad (66)$$

Since $\mathbf{H}_{CR} \in \mathbb{C}^{M \times (K_S-1)}$ and the matrix $[\mathbf{b}_1, \mathbf{H}_{CR}]$ is of full column rank, we have that $\dim(\Delta) = \dim(P_{\mathbf{b}_1}^\perp \mathbf{H}_{CR}) = K_S - 1$. Furthermore, it is easy to see that

$$\text{span}(P_{\mathbf{b}_1}^\perp \mathbf{H}_{CR}) \cap \text{span}(P_{\mathbf{b}_1}^\perp) = \emptyset, \quad (67)$$

then we have

$$\dim(P_\Delta^\perp P_{\mathbf{b}_1}^\perp) = M - \dim(\Delta) - \dim(P_{\mathbf{b}_1}^\perp) = M - K_S. \quad (68)$$

It follows from (65) and (67) that

$$\text{span}(P_{\mathbf{A}(\boldsymbol{\eta}_\theta)}^\perp) \subset \text{span}(P_\Delta^\perp P_{\mathbf{b}_1}^\perp) = \text{span}(P_{\mathbf{b}_1}^\perp P_\Delta^\perp). \quad (69)$$

It follows from (66), (68) and (69) that the projection matrixes $P_{\mathbf{b}_1}^\perp, P_\Delta^\perp P_{\mathbf{b}_1}^\perp$ and $P_{\mathbf{A}(\boldsymbol{\eta}_\theta)}^\perp$ span the same space. Consequently, (34) holds, which completes the proof of R6.

REFERENCES

- [1] H. Krim and M. Viberg, "Two decades of array signal processing research: the parametric approach," *IEEE Signal Process. Mag.*, vol. 13, no. 4, pp. 67–94, Jul. 1996.
- [2] P. Stoica and R. Moses, *Spectral Analysis of Signals*. Upper Saddle River, NJ, USA: Prentice-Hall, 2005.
- [3] F. Wen, Q. Wan, R. Fan, and H. W. Wei, "Improved MUSIC algorithm for multiple noncoherent subarrays," *IEEE Signal Process. Lett.*, vol. 21, no. 5, pp. 527–530, May 2014.

- [4] R. O. Schmidt, "Multiple emitter location and signal parameter," *IEEE Trans. Antennas Propag.*, vol. 34, no. 3, pp. 276–280, Mar. 1986.
- [5] S. U. Pillai and B. H. Kwon, "Forward/backward spatial smoothing techniques for coherent signal identification," *IEEE Trans. Acoust. Speech, Signal Process.*, vol. 37, no. 1, pp. 8–15, Jan. 1989.
- [6] D. M. Malioutov, "A sparse signal reconstruction perspective for source localization with sensor arrays," *IEEE Trans. Signal Process.*, vol. 53, no. 8, pp. 3010–3022, Aug. 2005.
- [7] P. Stoica, P. Babu, and J. Li, "SPICE: A novel covariance-based sparse estimation method for array processing," *IEEE Trans. Signal Process.*, vol. 59, no. 2, pp. 629–638, Feb. 2011.
- [8] J. Yin and T. Chen, "Direction-of-arrival estimation using a sparse representation of array covariance vectors," *IEEE Trans. Signal Process.*, vol. 59, no. 9, pp. 4489–4493, Sep. 2011.
- [9] S. D. Blunt and S. Member, "Robust DOA estimation: The reiterative superresolution (RISR) algorithm," *IEEE Trans. Aerosp. Electron. Syst.*, vol. 47, no. 1, pp. 332–346, Jan. 2011.
- [10] Z. Yang, L. Xie, and C. Zhang, "Off-grid direction of arrival estimation using sparse Bayesian inference," *IEEE Trans. Signal Process.*, vol. 61, no. 1, pp. 38–43, Jan. 2013.
- [11] D. P. Wipf and B. D. Rao, "An empirical Bayesian strategy for solving the simultaneous sparse approximation problem," *IEEE Trans. Signal Process.*, vol. 55, no. 7, pp. 3704–3716, Jul. 2007.
- [12] S. Y. Kung, C. Lo, and R. Foka, "A Toeplitz approximation approach to coherent source direction finding," in *Proc. IEEE Int. Conf. Acoust. Speech Signal Process.*, 1986, vol. 11, pp. 193–196.
- [13] H. Tao, J. Xin, J. Wang, and N. Zheng, "Two-dimensional direction estimation for a mixture of noncoherent and coherent signals," *IEEE Trans. Antennas Propag.*, vol. 63, no. 2, pp. 318–333, Jan. 2015.
- [14] X. Xu, Z. F. Ye, and Y. F. Zhang, "DOA estimation for uncorrelated and coherent signals with centre-symmetric circular array," *J. Univ. Sci. Technol. China*, vol. 39, pp. 1–5, 2009.
- [15] X. Xu, Z. F. Ye, Y. F. Zhang, and C. Q. Chang, "A deflation approach to direction of arrival estimation for symmetric uniform linear array," *IEEE Antennas Wireless Propag. Lett.*, vol. 5, no. 1, pp. 486–489, Dec. 2006.
- [16] Z. F. Ye and X. Xu, "DOA estimation by exploiting the symmetric configuration of uniform linear array," *IEEE Trans. Antennas Propag.*, vol. 55, no. 12, pp. 154–157, Dec. 2007.
- [17] F. Liu, J. Wang, C. Sun, and R. Du, "Spatial differencing method for DOA estimation under the coexistence of both uncorrelated and coherent signals," *IEEE Trans. Antennas Propag.*, vol. 60, no. 4, pp. 2052–2062, Apr. 2012.
- [18] Y. F. Zhang and Z. F. Ye, "Efficient method of DOA estimation for uncorrelated and coherent signals," *IEEE Antennas Wireless Propag. Lett.*, vol. 7, no. 3, pp. 799–802, 2008.
- [19] X. Xu, Z. F. Ye, and J. Peng, "Method of direction-of-arrival estimation for uncorrelated, partially correlated and coherent sources," *IET Microw., Antennas Propag.*, vol. 1, no. 4, pp. 949–954, 2007.
- [20] Z. F. Ye, Y. F. Zhang, X. Xu, and C. Liu, "Direction of arrival estimation for uncorrelated and coherent signals with uniform linear array," *IET Radar Sonar Navigat.*, vol. 3, no. 2, pp. 144–154, 2009.
- [21] C. Qi, Y. Wang, Y. Zhang, and Y. Han, "Spatial difference smoothing for DOA estimation of coherent signals," *IEEE Signal Process. Lett.*, vol. 12, no. 11, pp. 800–802, Nov. 2005.
- [22] P. Stoica and A. Nehorai, "Performance study of conditional and unconditional direction-of-arrival estimation," *IEEE Trans. Acoust. Speech, Signal Process.*, vol. 38, no. 10, pp. 1783–1795, Oct. 1990.
- [23] P. Stoica and K. C. Sharman, "Novel eigenanalysis method for direction estimation," *IEE Proc.*, vol. 137, no. 1, pp. 19–26, 1990.
- [24] A. B. Gershman and P. Stoica, "New MODE-based techniques for direction finding with an improved threshold performance," *Signal Process.*, vol. 76, no. 3, pp. 221–235, 1999.
- [25] C. Qian, L. Huang, N. D. Sidiropoulos, and H. C. So, "Enhanced PUMA for direction-of-arrival estimation and its performance analysis," *IEEE Trans. Signal Process.*, vol. 64, no. 16, pp. 4127–4137, Aug. 2016.
- [26] Y. F. Zhang, Z. F. Ye, and C. Liu, "Estimation of fading coefficients in the presence of multipath propagation," *IEEE Trans. Antennas Propag.*, vol. 57, no. 7, pp. 2220–2224, Jul. 2009.
- [27] H. Yan and H. H. Fan, "On source association of DOA estimation under multipath propagation," *IEEE Signal Process. Lett.*, vol. 12, no. 10, pp. 717–720, Oct. 2005.
- [28] Q. T. Zhang, K. M. Wong, P. C. Yip, and J. P. Reilly, "Statistical analysis of the performance of information theoretic criteria in the detection of the number of signals in array processing," *IEEE Trans. Acoust., Speech, Signal Process.*, vol. 37, no. 10, pp. 1557–1567, Oct. 1989.
- [29] T. J. Shan, A. Paulraj, and T. Kailath, "On smoothed rank profile tests in eigenstructure methods for directions-of-arrival estimation," *IEEE Trans. Acoust., Speech, Signal Process.*, vol. 35, no. 10, pp. 1377–1385, Oct. 1987.
- [30] Y. Bresler, "Maximum likelihood estimation of linearly structured covariance with application to antenna array processing," in *Proc. 4th Annu. ASSP Workshop Spectrum Estimation Model.*, 1988, pp. 1–4.
- [31] B. Hochwald and A. Nehorai, "Concentrated Cramér–Rao bound expressions," *IEEE Trans. Inf. Theory*, vol. 40, no. 2, pp. 363–371, Mar. 1994.
- [32] D. Wipf and S. Nagarajan, "Iterative reweighted l_1 and l_2 methods for finding sparse solutions," *IEEE J. Sel. Topics Signal Process.*, vol. 4, no. 2, pp. 317–329, Apr. 2010.
- [33] J. C. Ye, J. M. Kim, and Y. Bresler, "Improving M-SBL for joint sparse recovery using a subspace penalty," *IEEE Trans. Signal Process.*, vol. 63, no. 24, pp. 6595–6605, Dec. 2015.
- [34] I. Ziskind and M. Wax, "Maximum likelihood localization of multiple sources by alternating," *IEEE Trans. Acoust., Speech, Signal Process.*, vol. 36, no. 10, pp. 1553–1560, Oct. 1988.
- [35] P. Stoica and E. G. Larsson, "Comments on 'Linearization method for finding Cramér–Rao bounds in signal processing'," *IEEE Trans. Signal Process.*, vol. 49, no. 12, pp. 3168–3169, Dec. 2001.



Wei Xie (S'17) was born in Neijiang, Sichuan, China, in 1989. He received the B.S. degree in electronic information science and technology from Yantai University, Yantai, China, in 2011. He is currently working toward the Ph.D. degree in the Department of Electronic Engineering, University of Electronic Science and Technology of China, Chengdu, China. His research interests include array signal processing, sparse signal representation, and radio localization.



Fei Wen (M'15) received the B.S. degree and the Ph.D. degree in communications and information engineering from the University of Electronic Science and Technology of China, Chengdu, China, in 2006 and 2013, respectively. Since December 2012, he has been a Lecturer at the Air Force Engineering University, Xi'an, China. He is currently a Research Fellow with the Department of Electronic Engineering, Shanghai Jiao Tong University, Shanghai, China. His main research interests include statistical signal processing and nonconvex optimization.



Jiangbo Liu (S'17) received the B.S. degree in information and computing science from the Yanbian University, Jilin, China, in 2012. He is currently working toward the Ph.D. degree at the University of Electronic Science and Technology of China, Chengdu, China. His research interests focus on array signal processing especially the robust adaptive beamforming.



Qun Wan (M'04) received the B.Sc. degree in electronic engineering from Nanjing University, Nanjing, China, in 1993, the M.Sc. and Ph.D. degrees in electronic engineering from the University of Electronic Science and Technology of China (UESTC), Chengdu, China, in 1996 and 2001, respectively. From 2001 to 2003, he was a Postdoctoral Researcher with the Department of Electronic Engineering, Tsinghua University. Since 2004, he has been a Professor with the Department of Electronic Engineering, UESTC. He is currently the Director of the Joint Research Lab of Array Signal Processing and the Associate Dean of School of Electronic Engineering. His research interests include direction finding, radio localization, and signal processing based on information criterion.